MASTER IN CHEMISTRY PROFESSIONAL FOCUS

Design of novel copillar[4+1]arenes as ligands of SARS-CoV-2's spike protein

CORTINA, Florence

Award date:
2023

Awarding institution:
University of Namur

Université de Namur
Faculté des Sciences

Design of novel copillar[4+1]arenes as ligands of SARS-CoV-2's spike protein

Mémoire présenté pour l'obtention du grade académique de Master Chimie
« Chimie du Vivant et des Nanomatériaux » : Finalité Spécialisée en chimie en entreprise

Florence CORTINA

Janvier 2023

UNIVERSITE DE NAMUR
Faculté des Sciences
Secrétariat du Département de Chimie
Rue de Bruxelles 61 – 5000 NAMUR
Téléphone : +32(0)81 72.54.44 – Téléfax : +32(0)81 72.54.40
E-mail : enseignement.chimie@unamur.be - www.unamur.be/sciences

Conception de nouveaux copillar[4+1]arènes en tant que ligands de la protéine spike du SARS-CoV-2

CORTINA Florence

Résumé

En décembre 2019, l'émergence du virus SARS-CoV-2, un coronavirus humain hautement transmissible et pathogène, a entrainé des urgences sanitaires mondiales. Le mécanisme de liaison virus-hôte n'est pas encore tout à fait connu. Sa compréhension pourrait mener à de nouvelles stratégies antivirales.[1]

Un premier contact entre les virus et les cellules hôtes doit être établi avant tout lien avec le site de liaison des récepteurs. Les acides sialiques sont souvent utilisés par les coronavirus comme éléments de reconnaissance primaires. Cela initie l'entrée virale dans les cellules hôtes, par un procédé multi-étapes dans lequel le domaine de liaison du récepteur (RBD) de la glycoprotéine spike lie le récepteur hôte ACE2 (enzyme de conversion de l'angiotensine 2). Ensuite se produisent des changements conformationnels de la protéine spike, menant à la fusion des membranes virales et cellulaires.[1–4] Cela montre à quel point la protéine spike joue un rôle crucial dans l'infection par le virus.

Dans ce projet de recherche, nous nous concentrons sur la synthèse de structures hétéromultivalentes telles que les copillar[4+1]arènes, dans le but d'exploiter un effet multivalent et ainsi générer des ligands forts de la protéine spike du SARS-CoV-2 (Figure 1).[5] Des couplages orthogonaux avec des molécules biologiques, à savoir des dérivés d'acides sialiques, et des peptides spécifiques devraient permettre la conception de telles molécules antivirales.[6]

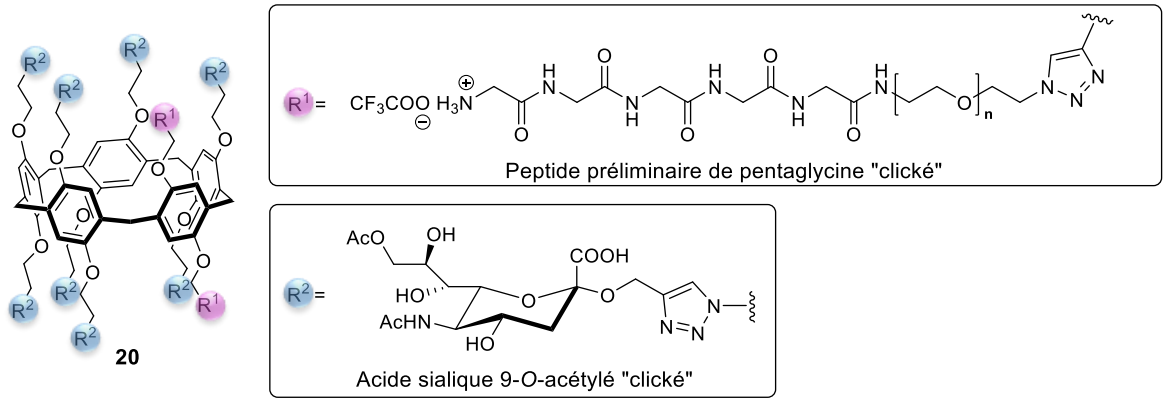

Figure 1 – Structure de la cible synthétique copillar[4+1]arène de ce projet de recherche

Mémoire de master en Sciences Chimiques à Finalité Spécialisée en chimie en entreprise
Janvier 2023

Promoteur : Prof. S. VINCENT

UNIVERSITE DE NAMUR
Faculté des Sciences
Secrétariat du Département de Chimie
Rue de Bruxelles 61 – 5000 NAMUR
Téléphone : +32(0)81 72.54.44 – Téléfax : +32(0)81 72.54.40
E-mail : enseignement.chimie@unamur.be - www.unamur.be/sciences

Design of novel copillar[4+1]arenes as ligands of SARS-CoV-2's spike protein

CORTINA Florence

Abstract

In December 2019, the emergence of SARS-CoV-2, a highly transmissible and pathogenic human coronavirus, led to global public health emergencies. The mechanism of the virus-host binding is still not fully known. Its understanding could lead to novel anti-viral strategies.[1]

A first contact between viruses and host cells needs to be made before any link with receptors binding site. Sialic acids are often used by coronaviruses as primary recognition elements. This initiates viral entry into host cells, by a multi-step process in which the Receptor Binding Domain (RBD) of the spike glycoprotein binds the host ACE2 (Angiotensin Converting Enzyme 2) receptor. Then, conformational changes of the spike protein occur, leading to the fusion of viral and cellular membranes.[1–4] This reveals that the spike proteins play a crucial role in virus infection.

In this project, we focus on the synthesis of heteromultivalent scaffolds such as copillar[4+1]arenes to exploit a multivalent effect to generate strong ligands of the SARS-CoV-2 spike protein (Figure 2).[5] Orthogonal couplings with biologically molecules namely sialic acid derivatives and specific peptides should achieve the design of such anti-viral molecules.[6]

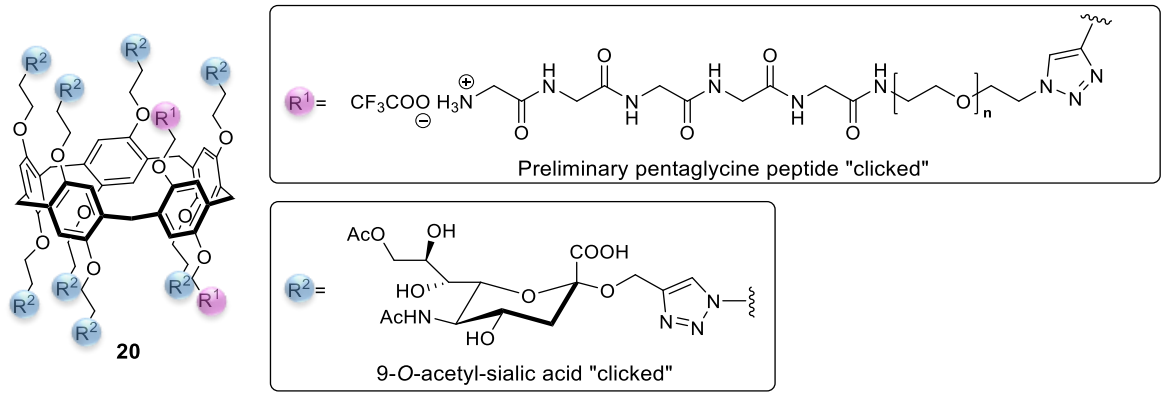

Figure 2 - Copillar[4+1]arene's structure as synthetic target of this research project

Mémoire de master en Sciences Chimiques à Finalité Spécialisée en chimie en entreprise
Janvier 2023

Promoteur : Prof. S. VINCENT

Remerciements

Je tiens à remercier en premier lieu le Professeur Stéphane Vincent de m'avoir offert l'opportunité de travailler sur un projet de mémoire aussi riche que passionnant, au sein de son laboratoire. Alors que son emploi du temps était fort rempli, il s'est toujours montré disponible pour m'orienter dans mes recherches, avec des conseils avisés.

Je tiens également à remercier mes encadrants, Dr. Kévin Renault et Jenny Ha, pour les nombreux moments passés à mes côtés au laboratoire. Ils m'ont, dès le début, poussé à m'améliorer et m'ont apporté de bons conseils. Grâce à leur expertise, j'ai pu développer mes compétences, tant au point de vue pratique que théorique.

Je souhaiterais remercier toute la team CBO pour leur accueil dans l'équipe et pour l'enthousiasme apporté par la personnalité de chacun. C'est aussi avec vous, Nacho, Marine, Arnaud, Loïc, Dmytro, Léa, Timothé, Jun et Maha, que j'ai passé cinq jours mémorables chaque semaine. Un merci particulier à Nacho pour la richesse de nos conversations au sein du CBO3.

Je me dois aussi de remercier mes deux camarades de mémoire, Rym et François, pour le trio que nous avons formé durant ces dix mois de challenges. Nous avons pu tisser des liens forts et su nous soutenir dans les moments plus difficiles.

Cette liste de remerciements ne serait pas complète sans y citer mes parents, sans qui je n'aurais pu mener à bien ces études. Ils m'ont toujours montré leur soutien, de par leurs petites attentions.

Je voudrais, finalement, remercier Clément d'avoir été à l'écoute et de m'avoir toujours soutenue durant ces dernières années.

Abbreviations and symbols

Ac_2O	Acetic anhydride
CH_3CN	Acetonitrile
AcCl	Acetyl chloride
Å	Angström
ACE2	Angiotensin-Converting Enzyme 2
$BF_3.Et_2O$	Boron trifluoride diethyl etherate
CBr_4	Carbon tetrabromide
δ	Chemical shift
COVID-19	Coronavirus disease 2019
$CuSO_4$	Copper(II) sulfate
CuAAC	Copper-catalysed Alkyne-Azide Cycloadditions
DCE	1,2-Dichloroethane
DCM	Dichloromethane
Et_2O	Diethyl ether
DMAP	*N*,*N*-dimethyl-4-aminopyridine
DMSO	Dimethyl sulfoxide
DMF	*N*,*N*-Dimethylformamide
DMB	1,4-Dimethoxybenzene
EtOAc	Ethyl acetate
Eq.	Equivalent
IC_{50}	Half-maximal inhibitory concentration
HCoV	Human Coronaviruses
J	Coupling constant
LiOH	Lithium hydroxide
m. p.	Melting point
mRNA	Messenger RNA
MeOH	Methanol
mM	Millimolar

μM	Micromolar
MS	Molecular Sieve
nM	Nanomolar
NMR	Nuclear Magnetic Resonance
S_N1	First order nucleophilic substitution
S_N2	Second order nucleophilic substitution
9OAc-SA	9-*O*-acetyl-sialic acid
p-TsOH	Para toluenesulfonic acid
$(CH_2O)_n$	Paraformaldehyde
ppm	Parts per million
K_2CO_3	Potassium carbonate
RBD	Receptor Binding Domain
RNA	Ribonucleic Acid
r. t.	Room temperature
R_F	Retention factor
SA	Sialic Acid
S protein	Spike protein
SARS-CoV-2	Severe Acute Respiratory Syndrome Coronavirus 2
AgOTf	Silver triflate
NaAsc	Sodium ascorbate
NaN_3	Sodium azide
NaOH	Sodium hydroxide
NaOMe	Sodium methoxide
TLC	Thin Layer Chromatography
TMPRSS2	Transmembrane Serine Protease 2
PPh_3	Triphenylphosphine
H_2O	Water

Table of contents

I. Introduction

I.1 SARS-CoV-2 virus

I.1.1 Coronaviruses

On December 2019, started the pandemic of COVID-19 in Wuhan (China), which was initially considered to be a severe pneumonia.[7] This disease was found to be caused by a virus called SARS-CoV-2 (Severe Acute Respiratory Syndrome Coronavirus 2). Accordingly, this virus was found to be a coronavirus, from the *Coronavirinae* subfamily in the *Coronaviridae* family. Coronaviruses are positive-stranded RNA viruses that infect a wide variety of mammalian and avian species.[7,8]

Human coronaviruses are known since the mid-1960s. We can distinguish seven human coronaviruses and all of them seem to have animal origins: SARS-CoV, SARS-CoV-2, MERS-CoV, HCoV-NL63 and HCoV-229E are thought to originate in bats while HCoV-OC43 and HCoV-HKU1 are likely to originate in rodents.[7,9] The transmission of the virus to humans may have happened *via* domestic animals, playing a role of intermediate hosts.[9] Human coronaviruses exhibit a common structure (Figure 3).[7] These viruses contain viral RNA packed by the nucleocapsid proteins (N) into the capsid. Envelope (E) and membrane (M) proteins are involved in the viral assembly and budding.[7,10] As many viruses, human coronaviruses display a glycoprotein on their surface. This spike protein (S protein) mediate their entry into host cells. Therefore, the S protein plays a crucial role in virus infection.[11]

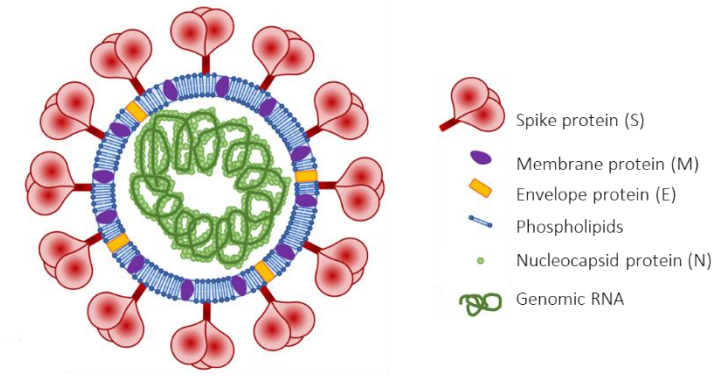

Figure 3 – Coronaviruses schematic structure[12]

I.1.2 Spike protein

The coronavirus spike protein, a glycoprotein protruding from the viral surface, is essential for the infectivity and host recognition (Figure 4).[7,13] In the case of SARS-CoV-2, the S protein is divided into two subunits: S1 and S2. The first subunit (S1) forms the head of

the spike and hosts the receptor biding domain (RBD). S1 facilitates viral attachment to target cells *via* its receptor binding domain, by binding the host ACE2 (angiotensin-converting enzyme 2) receptor. The ACE2 receptor is located on the human cells' surface and more specifically on the surface of lung alveolar epithelial cells and enterocytes of the small intestine.[14] In human cells, regulation of blood pressure and other cardiovascular functions, like heart and kidney regulation are functions provided by the ACE2 receptor.[2,15] The second subunit (S2) allows conformational changes of the spike glycoprotein, once cleaved by a host protease, and makes possible the fusion between the viral and cellular membranes.[3,16] S2 forms the stalk, which anchors the glycoprotein to the viral envelope, composed of three joints: the hip, knee and ankle. A degree of flexibility of spike protein is allowed by unusual hinge bending movements of these joints, which are movements along one plane. This flexibility allows the simultaneous action of several spike proteins from the same virus particle to bind one human cell.[13,17] This glycoprotein is coated in glycans, which makes it nearly invisible to the human immune system.[17,18]

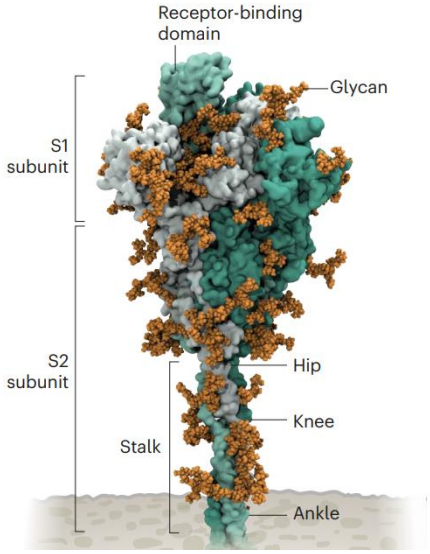

Figure 4 – Spike protein's structure, a hidden glycoprotein[17]

SARS-CoV-2 virus is known for its high infectivity. This activity can be explained for two reasons. Firstly, human cells are strongly bound by the virus (two or four times more than its predecessor, SARS-CoV).[19] Secondly, SARS-CoV-2 has the particularity to shut down the cell's alarm system. In fact, the virus suppresses the translation of host mRNA and thus prevent the production of host proteins, called interferons, responsible for alerting the immune system. This suppression happens once the virus begins translating its genome into viral proteins, which

will recruit host proteins to eliminate host mRNA. For those reasons, it is difficult for the immune system to fight against the virus.[17]

I.1.3 Infection cycle

Viruses need to pass through the glycocalyx of cells' surface, composed of a dense mixture of glycans, before engaging their receptors to mediate the entry into the target cell. Therefore, an evolution of many viruses has allowed them to employ glycans as co-receptors to make initial contact with target cells.[20] Although some coronaviruses are known to use sialic acids as primary recognition elements, the specific binding of SARS-CoV-2 to sialic acid has been debated.[18,21] Sialic acids, are nine-carbon sugar neuraminic acid derivatives located at the end of cell surface oligosaccharides.[5] It was demonstrated in the Prof. Vincent laboratory, in collaboration with Prof. Alsteens (UCLouvain), that 9-*O*-acetyl-sialic acid (9OAc-SA) displays a better affinity for the SARS-CoV-2 spike protein compared to sialic acid (Figure 5).[5,20]

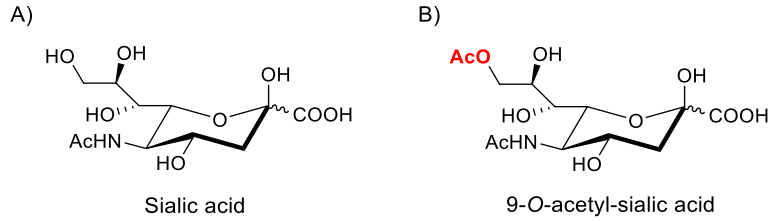

Figure 5 – Schematic representation of A) sialic acid (called N-acetyl-neuraminic acid) - B) 9-O-acetyl sialic acid

So, sialic acids are carbohydrates and exhibits two possible diasteroisomers (α and β), which can be differentiated by the substituent's configuration (equatorial or axial) at the 2-position, named anomeric carbon (Figure 6). Depending on the conformation of the carbohydrate chair ($^1C_4$ or $^4C_1$), the axial substituent at the 2-position is in α or β configuration. The α anomer of carbohydrates in $^1C_4$ conformation presents an equatorial substituent at the 2-position, and the β anomer presents an axial substituent at the 2-position. The contrary is true for $^4C_1$ conformation: α anomer displays an axial substituent at the 2-position and β anomer displays an equatorial substituent at the 2-position.[22] In this project research, all carbohydrates schemes are drawn in the more stable $^1C_4$ conformation.

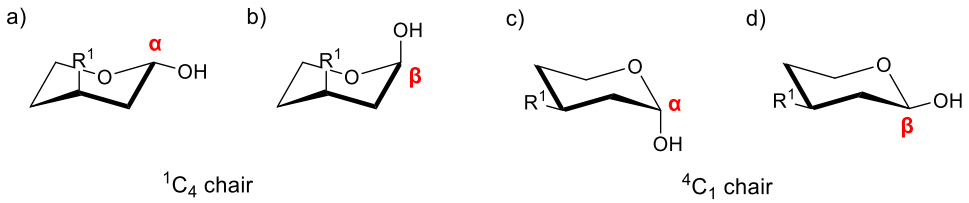

Figure 6 – Schematic representation of possible diasteroisomers for the two carbohydrates conformation - a) α anomer for $^1C_4$ chair - b) β anomer for $^1C_4$ chair - c) α anomer for $^4C_1$ chair - d) β anomer for $^4C_1$ chair

In carbohydrates, there is a phenomenon, called anomeric effect, in which the electronegative substituent (X= halogens, OR, OAc, SR, etc.) in the 2-position (anomeric carbon) is preferentially axial. An overlap of one endocyclic oxygen atom lone pair with the antibonding molecular orbital σ^* of the C-X bond stabilizes this electronegative substituent, when axial. These two orbitals have to be parallel to each other (Figure 7).[22]

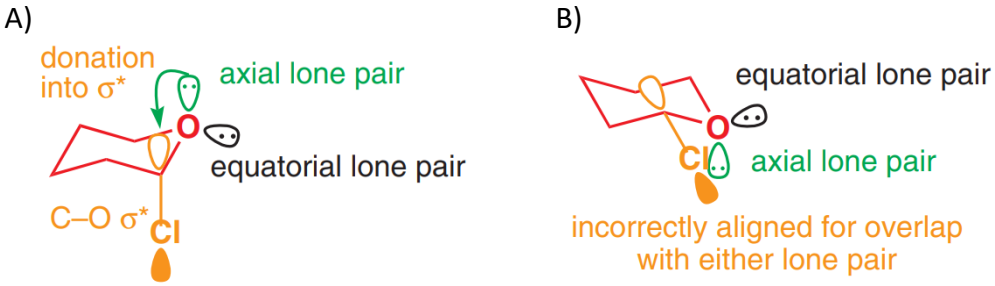

Figure 7 – Schematic representation of the anomeric effect present in A) and not present in B)[22]

The steps following the entry of the virus into host cells are not fully understood as it is more difficult to observe what happens at the cell level.[17] Once the ACE2 receptor is bound by the virus *via* the spike protein S1 subunit, the entry of the virus in the cytosol is allowed by endocytosis (Figure 8). Indeed, a proteolytic activation occurs, where the S2 subunit is cleaved from the S1 subunit, by the host protease TMPRSS2 (Transmembrane Serine Protease 2). This proteolytic activation results in the exposure of some hydrophobic amino acids that bury themselves in the host cell membrane, leading to the merging of viral and cell membranes (Figure 9).[1,23] Immediately after the entry of the virus by endocytosis, the viral RNA (genome) is released into the host cytosol. The viral RNA is sequenced in a particular manner. The amino acids sequence is constituted of two major parts. The amino acids in the first part are coding for non-structural proteins and the ones in the second part are coding for structural proteins. The first part of the genome sequence is translated by ribosomes into non-structural proteins, such as viral polymerase which enables genome replication.[3,12] The second part of the genome sequence is translated into structural proteins, such as spike, membrane and envelope proteins.

All these proteins then transit through the endoplasmic reticulum-Golgi pathway to generate virions. These new virions are then released from the host, by exocytosis and are generated to produce more virus particles to infect more and more cells.[2,4]

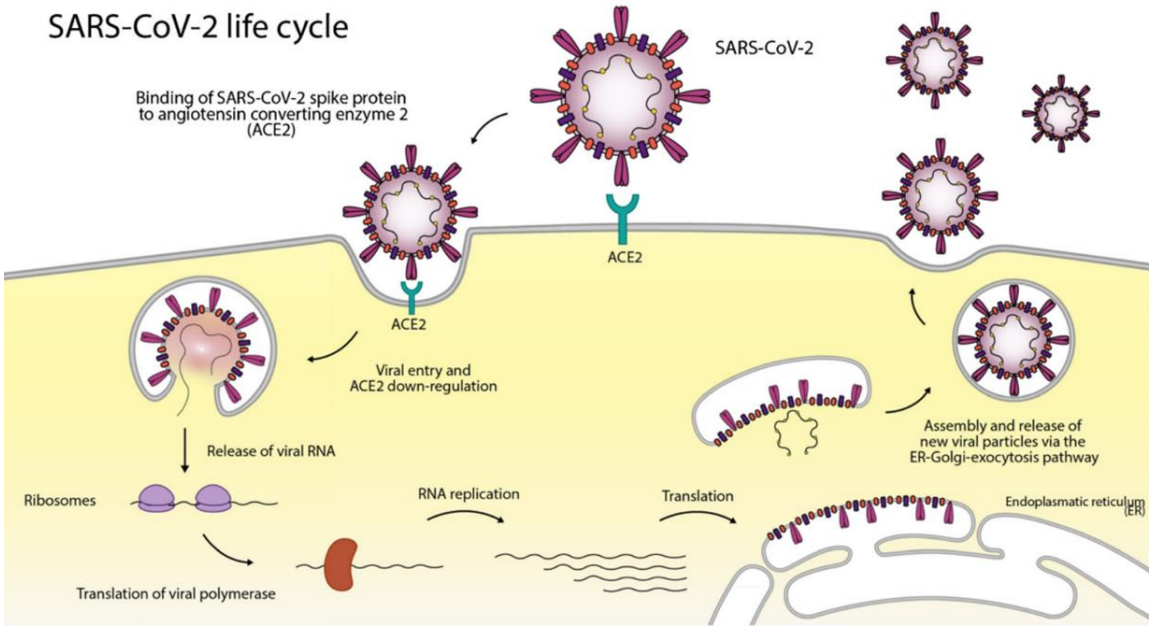

Figure 8 - Schematic view of SARS-CoV-2's life cycle[3]

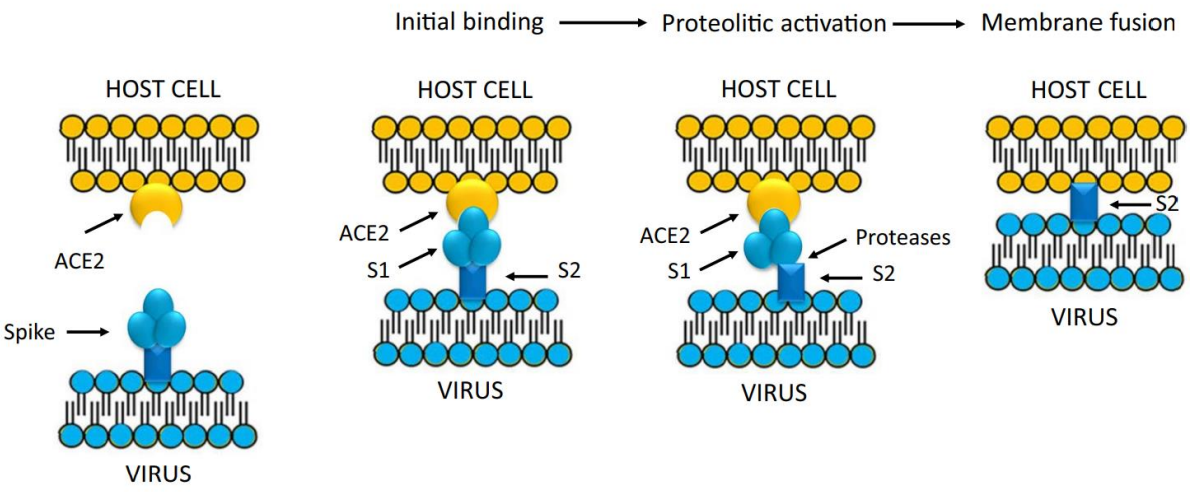

Figure 9 – Scheme of the membrane fusion process initiating SARS-CoV-2 infection cycle[23]

I.2 Multivalent effect

SARS-CoV-2 spike proteins play a crucial role in virus infection, using host ACE2 as a receptor and 9OAc-SA as co-receptor. However, the affinity between the spike protein and its ligands is generally weak (in the mM range), especially for carbohydrates, such as sialic

acids.[25] This weak affinity is compensated by a strong local free ligand concentration during the lung infection.[21] Chemists get inspired from this natural phenomenon to create objects able to reproduce this enhancement of affinity, which is the so-called multivalent effect. In this multivalent effect, the affinity of a given ligand with a receptor can be dramatically enhanced if the ligand is locally concentrated.[26,27] There are five possible multivalent effects (Figure 10):

(A) Chelate effect: simultaneous multiple interactions of a multivalent ligand with several receptors.
(B) Clustering effect: receptors cluster together when approaching a multivalent ligand.
(C) Steric stabilization: the binding of multivalent ligands prevents the binding of another compound, by their size.
(D) Subsite binding: presence of several binding sites on receptors.
(E) Statistical effect: the multivalent ligand slides along the receptors.

The binding of a multivalent ligand towards a receptor can be enhanced by one or more of these five multivalent effects.

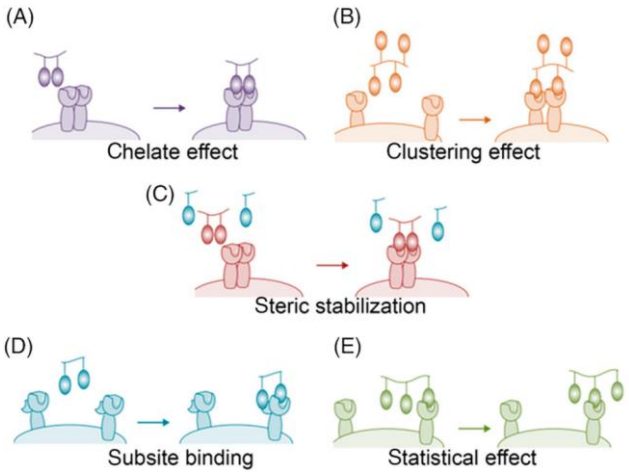

Figure 10 – Schematic representation of the five multivalent effects[27]

I.3 Macrocycles

I.3.1 Generalities

Great interest has been shown in macrocycles because of their many potential applications including ion transport, catalysis, medicines synthesis, drug delivery, food processing, molecular machines etc.[28,29] Macrocycles are particularly attractive molecules in this study. Indeed, macrocycles are exploited during the past decade as ideal platform for

multivalent scaffold development.[30] These molecules are mainly known in the field of supramolecular chemistry, performing non-covalent host-guest interactions with their cavities.[31] Cyclodextrins, calixarenes, cucurbiturils and crown ethers are four of the most well-known macrocycles and some were even discovered as early as the 19th century.[31] Recently, a new generation of macrocycles has been discovered: pillar[n]arenes.[32]

I.3.2 Pillar[n]arenes

Pillar[n]arenes are a new class of macrocyclic compounds, synthetized by serendipity by Tomoki Ogoshi and co-workers in 2008. The resulting compound was named DMpillar[5]arene due to the starting material used, the DMB (1,4-dimethoxybenzene).[32] Pillar[n]arenes are macrocycles composed of several dialkoxybenzene units, linked together by methylene bridges at *para* position. The number of repeating units (n) ranges from 5 to 10 (Figure 11).

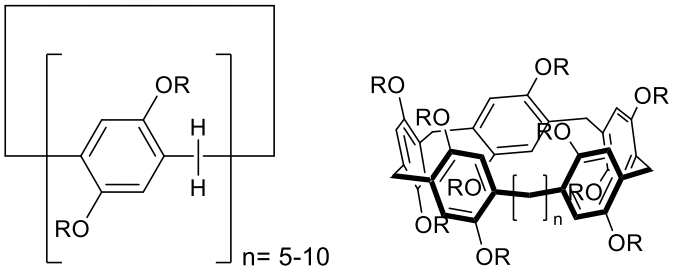

Figure 11 – Two possible schematic representations of pillar[n]arenes

Pillar[n]arenes synthesis can proceeds under thermodynamic or kinetic control. Pillar[5]arenes and pillar[6]arenes syntheses are the only one proceeding by thermodynamic control, which are directed by template effect. This effect relies on non-covalent interactions in which the reaction solvent controls the synthesis (Figure 12). Indeed, oligomerization of monomer precursors around the solvent molecule occurs to form the macrocycle. The solvent choice is crucial as the size of the solvent directly impacts on the size of the pillar[n]arene and on whether or not cyclization takes place. Bulky hydrocarbon molecules such as chlorocyclohexane acts as template solvent for pillar[6]arenes synthesis.[33] The solvent used to synthetize pillar[5]arene is dichloroethane, which size perfectly fits to be included in the pillar[5]arene's cavity. However, chloroform does not enable pillar[5]arene synthesis as the solvent molecule size is too large.[30] In fact, chloroform is used to the synthesis of larger pillar[n]arenes (n =7-10), which occurs under kinetic control and do not benefit from the template effect. So, reaction time needs to be carefully selected for each pillar[7-10]arene.[34]

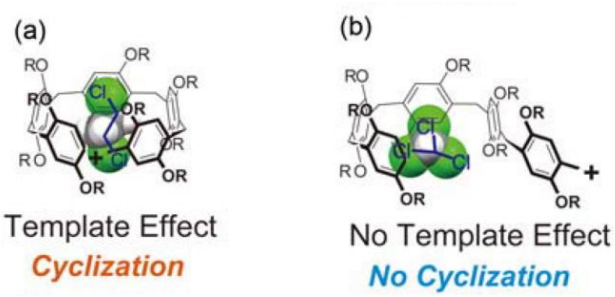

Figure 12 –Template effect for pillar[5]arene[30]

Pillar[5]arenes have immediately attracted the interest of scientists and they are already playing a major role in supramolecular chemistry. In fact, pillar[5]arenes are the most studied as the synthesis is the easiest one, leading to highest yields (> 80%). Pillar[6]arenes are also widely used, giving good yields (> 70%). However, the synthesis of pillar[7-10]arenes leads to low yields (< 5%).[34] As the syntheses of pillar[7-10]arenes are kinetically controlled, various pillar[n]arenes are formed, which explains the lower yields than pillar[5]arenes synthesis.[33,35] Furthermore, pillar[n]arenes display three advantages compared to other macrocycles. Firstly, selective binding to guests is ensured by the high symmetry of pillar[n]arenes. Second, host-guest properties can be tuneable thanks to their versatile functionalization. Finally, pillar[n]arenes are soluble in organic solvents, which complements the other macrocycles water-soluble, such as cucurbiturils and cyclodextrins.[36]

Various applications have already been found, such as drug delivery systems, supramolecular catalysis, multivalent recognition, artificial water channels, molecular sensor etc.[29] Indeed, they have unique structural features, which further develops this field in chemistry.[37]

1) Totally symmetrical pillar shape: pillar[5]arenes' is a one dimensional pentagon structure (Figure 13).[32]
2) π-electron rich cavity: pillar[5]arene is composed of five electron-rich dialkoxybenzene units and the *para*-methylene bridges force the rings to face each other, it leads to a π-electron rich cavity (Figure 13).[38] Pillar[5]arene can therefore form host-guest complexes with electron-accepting molecules and linear neutral molecules, such as viologen and n-hexane, respectively.[36]

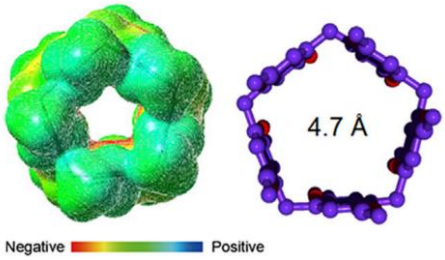

Figure 13 – Calculated electron-potential profile and cavity size of pillar[5]arene[38]

3) Versatile functionalization: the dialkoxybenzene units increase the molecular diversity by their functionalization.[39]
4) High biocompatibility: pillar[n]arenes are molecules readily accepted by biological media, performing with an appropriate host response in a specific application.[36,40]
5) Planar chirality: the substituents are not perpendicular to the methylene bridge linkages, each unit in pillar[n]arenes can rotate along these bonds and generate conformational isomers (Figure 14).[41]

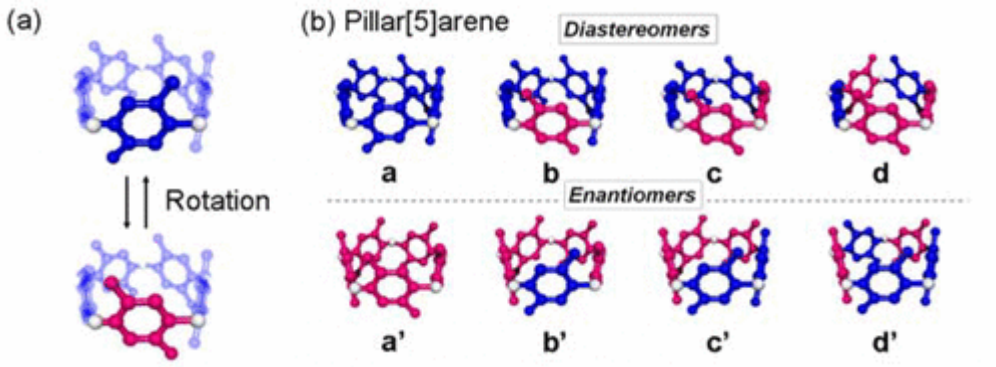

Figure 14 – a) Rotational mode of the dialkoxybenzene units of pillar[5]arene – b) Planar chirality of pillar[5]arenes[30]

In a homopillar[5]arene, all five dialkoxybenzene units are the same. However, if one dialkoxybenzene unit differs from the others, the compound is called a copillar[4+1]arene. If two units differ from the others, the compound is called a copillar[3+2]arene (Figure 15).[29,42] Prof. Vincent laboratory has been recently interested in the synthesis of copillar[4+1]arene to generate multivalent scaffolds functionalized at one arene unit of the copillar.[6,20] Indeed, copillar[4+1]arenes provide molecular diversity and functionalization of different objects on one scaffold.

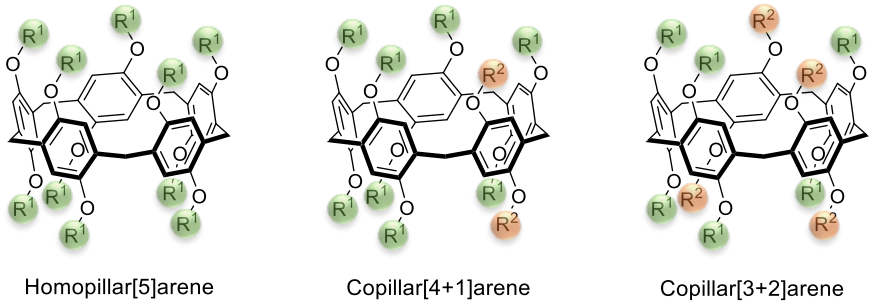

Figure 15 - Different types of pillar: homopillar[5]arene, copillar[4+1]arene and one isomer of copillar[3+2]arene

There are two types of multivalent ligands: homomultivalent and heteromultivalent. As proof of concept, an homomultivalent scaffold based on pillar[5]arenes functionalized with 9OAc-SA was used successfully for SARS-CoV-2 neutralization.[5] Indeed, targeting the 9OAc-SA binding site on spike protein can be an efficient way to inhibit infection.[20,43] The 9OAc-SA exhibits a satisfying IC_{50} value, above 100 μM.[5] However, the 9OAc-SA on a multivalent scaffold (called glycocluster) such as pillar[5]arene has a better IC_{50}, in the range of 1-10 μM, confirming the multivalent effect.[5] Moreover, focusing also on the ACE2 receptor may inhibit SARS-CoV-2 infection. According to the literature, ACE2-derived peptides are used for this purpose.[44] The IC_{50} displayed by these peptides is in the μM range while the binding affinity of the RBD with the host ACE2 receptor is 120 nM (measured by atomic force microscopy).[20] Interestingly, recent studies have shown that the sialic acid binding site on S protein and the ACE2 binding pocket might not overlap. If both binding pockets are simultaneously occupied, there may exist an heteromultivalent effect from the inhibition point of view.[20] This shows the appeal of heteromultivalent scaffolds such as copillar[4+1]arenes.

There are two possible copillar[4+1]arenes A and B targeted in this project research (Figure 16). The first one is composed of two 9OAc-SA and eight peptides (copillar[4+1]arene A) and the second one is composed of eight 9OAc-SA and two peptides (copillar[4+1]arene B). As the IC_{50} is the concentration of an inhibitor needed to inhibit a biological process by 50%, the lower the IC_{50}, the better the inhibition. The IC_{50} of ACE2-derived peptide (μM range) is lower than the one of 9OAc-SA (above 100 μM). It is not necessary to functionalize eight peptides on the copillar[4+1]arene as the IC_{50} is good enough. However, the IC_{50} displayed by 9OAc-SA is high, so it is mandatory to functionalize more 9OAc-SA on the copillar[4+1]arene to benefit from the multivalent effect. The IC_{50} of 9OAc-SA will therefore be reduced (to 1-10 μM). In summary, the copillar[4+1]arene B is the best potential antiviral candidate among both.

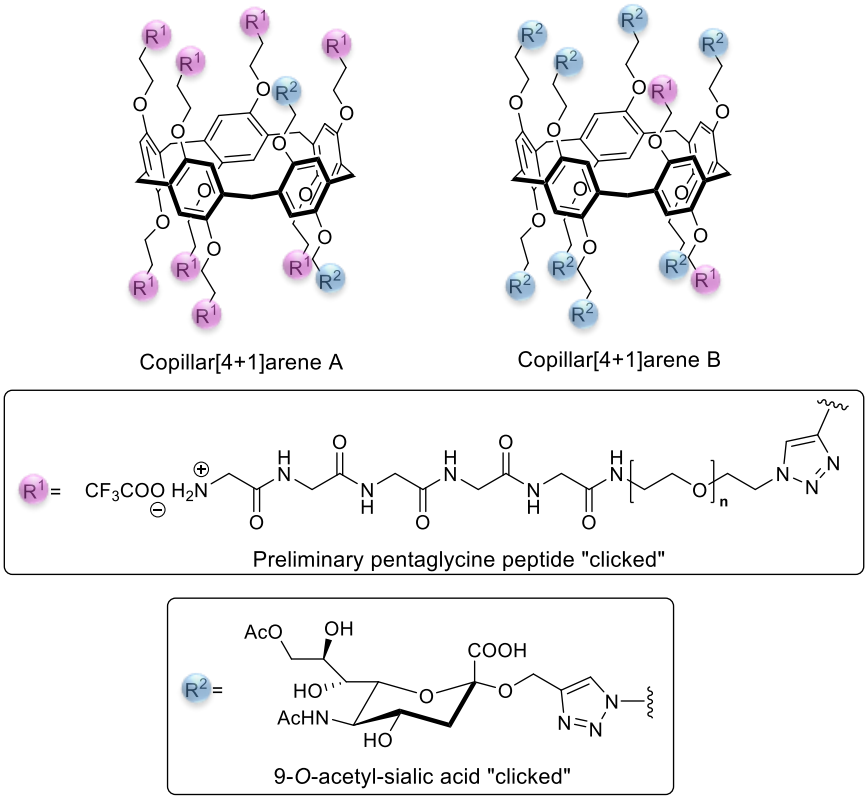

Figure 16 – The two possible structures of copillar[4+1]arenes A and B

The reasons why we selected a pentaglycine peptide in copillar[4+1]arene B (R^1 group in Figure 16) will be explained in the next section.

II. Objectives

The overall objective of this project is the development of copillar[4+1]arene **20** as a heteromultivalent scaffold to interrupt the binding process of SARS-CoV-2's spike protein to host cells, at an early stage (Figure 17). Specifically, this means that the interruption of binding will take place before the cleavage of the spike protein which normally leads to the entry of the virus into host cells. [20,44]

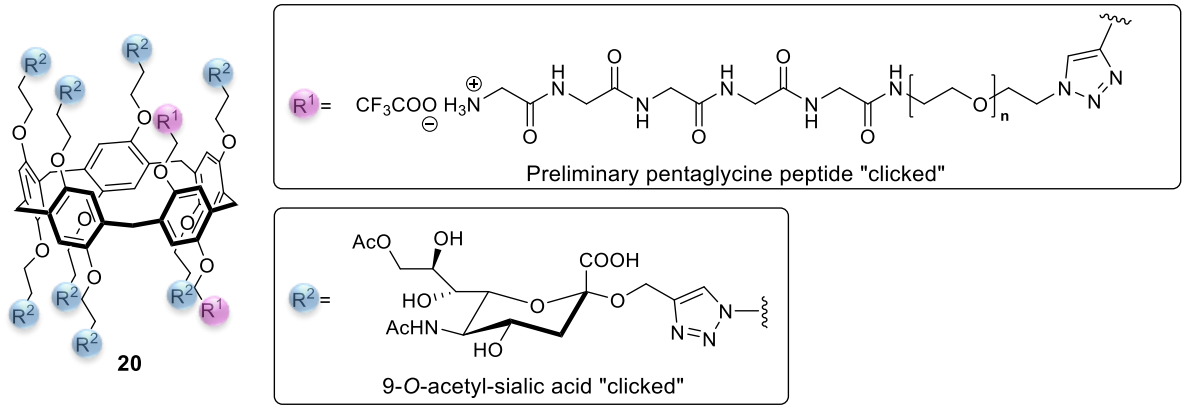

*Figure 17 - Copillar[4+1]arene's **20** structure as synthetic target of this research project*

The final copillar[4+1]arene's **20** retrosynthetic pathway is presented in Scheme 1. Orthogonal couplings, by copper-catalysed alkyne-azide cycloaddition (CuAAC), with 9OAc-SA and specific peptides should achieve the design of such anti-viral molecules.[6]

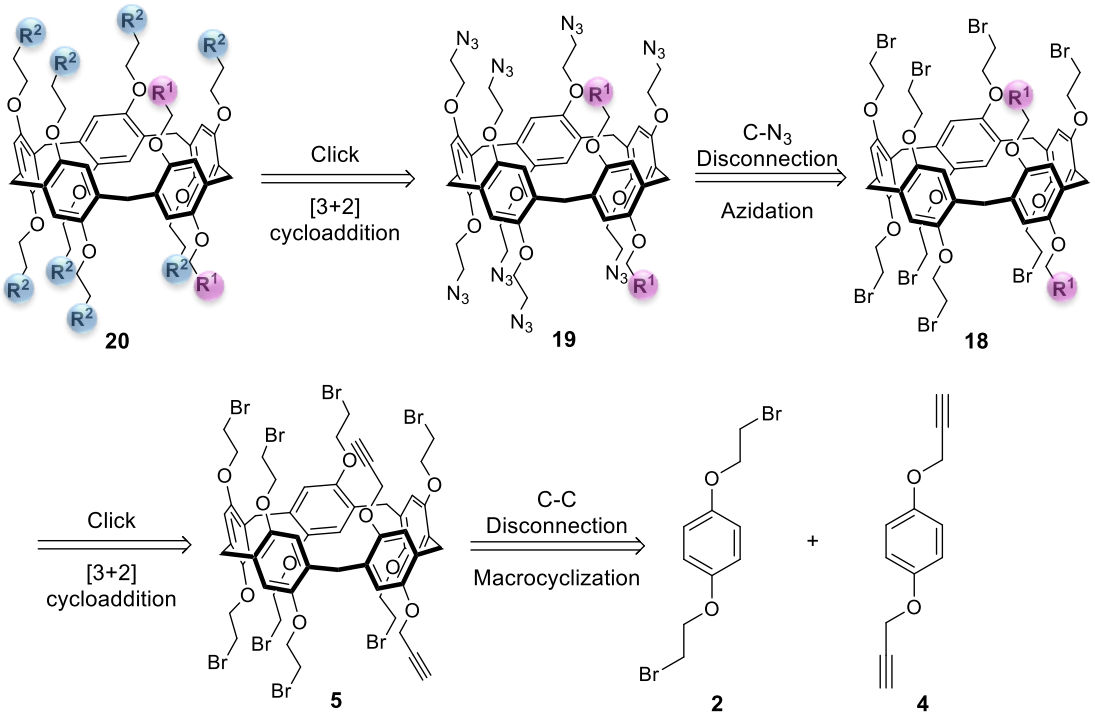

*Scheme 1 – Retrosynthetic pathway of the target copillar[4+1]arene **20***

CuAAC is a cycloaddition reaction based on Huisgen 1,3-dipolar cycloaddition, which makes react a molecule carrying an alkyne with another carrying an azide to ligate both through a triazole formation. However, there is a difference between both of these cycloadditions. CuAAC is copper(I)-catalyzed, while Huisgen 1,3-dipolar cycloaddition is not. Copper-catalysed alkyne-azide cycloaddition is fast and high-yielding reaction, so that it belongs to the ensemble of "click reactions" (Figure 18). The catalytic process also offers the advantage to regiospecifically generate the 1,4 regioisomer triazole.[45]

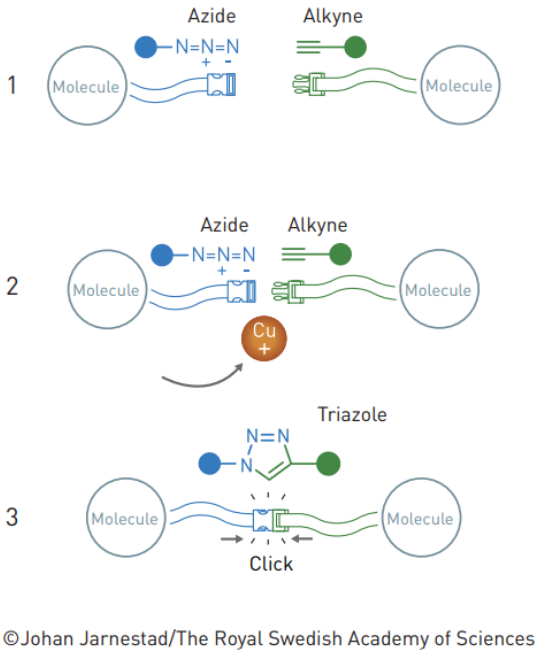

Figure 18 – Schematic representation of a CuAAC reaction (click chemistry)[46]

Once the final copillar[4+1]arene **20** synthesis is achieved, the functionalization of ACE2-dervied peptides (structure is still confidential) needs to be performed. Indeed, these peptides can be used to mimic the host ACE2 receptor used by SARS-CoV-2 to enter into host cells.[1] As a preliminary pentaglycine peptide is present on the copillar[4+1]arene **20**, a sortase-mediated ligation reaction can be performed, to achieve ACE2-derived peptides' functionalization. This enzymatic reaction consists in a transfer of the LPXTG motif, carried by a substrate protein to an aminoglycine nucleophile, through a sortase.[47] This leads to the ligation of the substrate protein and the aminoglycine peptide (Figure 19). In other words, such a strategy may allow to graft virtually any peptide to copillar[4+1]arene **20** scaffold, as long as it bears the signal LPXTG motif.

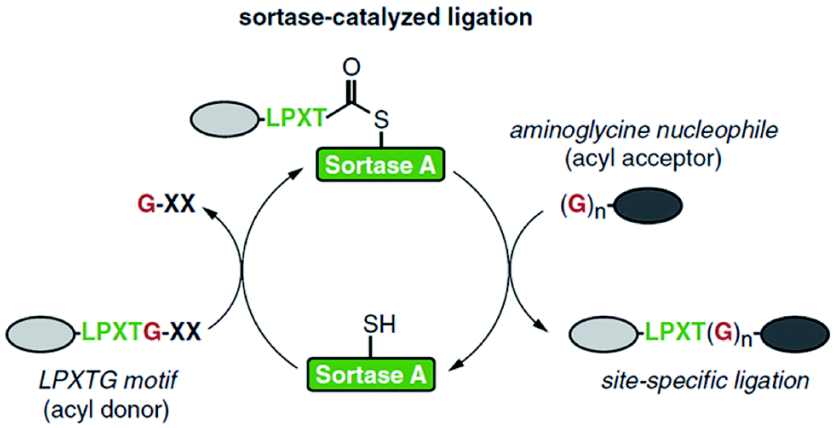

Figure 19 - Catalytic cycle of sortase-mediated ligation [47]

As the project is quite ambitious, we focused on the synthesis of the central scaffold (copillar[4+1]arene **5**) and of 9-*O*-acetyl-sialic acid (9-OAc-SA). On one hand, copillar[4+1]arene synthesis is known to be rather complicated, giving low yields and leading to purification difficulties.[34,48] A methodological work is probably necessary to optimize the copillar[4+1]arene **5** synthesis. The design of this scaffold is possible by a cyclization reaction between two different monomers: 1,4-bis(2-bromoethoxybenzene) **2** and 1,4-bis(2-propargyloxybenzene) **4**. On the other hand, the synthesis of 9OAc-SA is possible through a multi-step pathway from *N*-acetyl-neuraminic acid. Moreover, the stereoselective installation of a propargyl group onto the sialic acid will be a really crucial step as only the α diasteroisomer has to be isolated, in a pure form. So, a α/β mixture separation will have to be performed, probably requiring a methodological work.

III. Results and discussion

III.1 Synthesis of copillar[4+1]arene

Initial efforts focused on synthesizing the copillar[4+1]arene pattern. The first reactions carried out were the synthesis of reagents **2** and **4** which are the copillar[4+1]arene **5** precursors. Compound **2** was synthetized by Appel reaction from 1,4-bis(2-hydroxyethoxybenzene) **1** with 93% yield. In parallel, compound **4** was synthetized with an excellent 98% yield by nucleophilic substitution of propargyl bromide by hydroquinone **3** under basic conditions (Scheme 2).

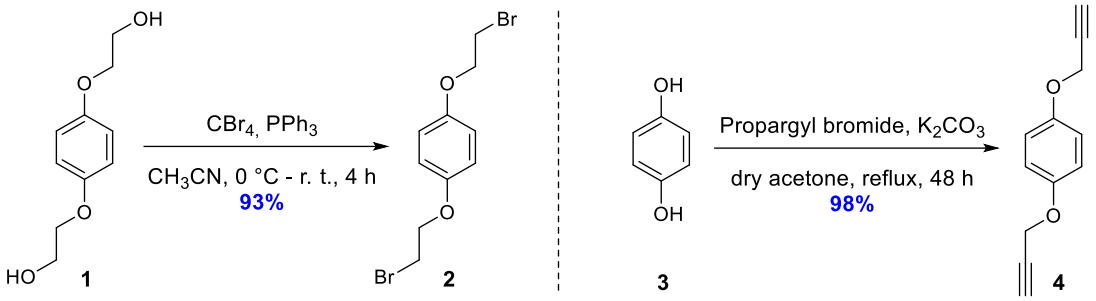

*Scheme 2 - Synthesis of the 1,4-bis(2-bromoethoxybenzene) **2** and the 1,4-bis(2-propargyloxybenzene) **4***

With these two reagents in hands, the synthesis of the copillar[4+1]arene **5** can be carried out (Scheme 3). This synthesis leads to modest yields and give several by-products such as homopillar[5]arene and polymers (composed of 1,4-bis(2-bromoethoxybenzene) **2**).[48] Indeed, the copillar[4+1]arene **5** is formed as the minor product. The major product formed is the pillar[5]arene, with a ratio copillar/pillar of 35/75. In this context, a methodological study needs to be done to optimize the synthesis of copillar[4+1]arene **5**. Several purification conditions have been tested and all attempts are summarized in the Table 1.

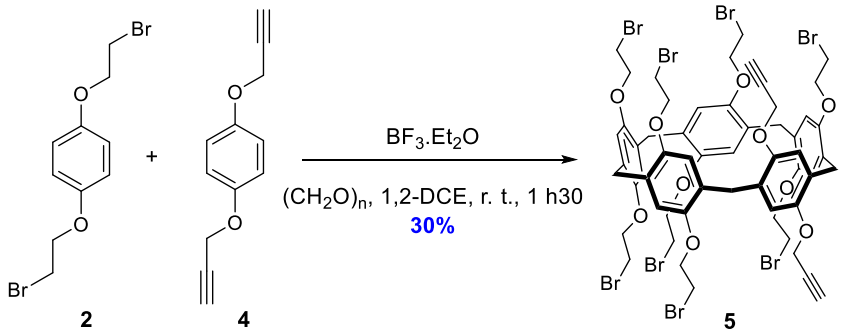

*Scheme 3 - Synthetic pathway of the copillar[4+1]arene **5***

For the initial conditions, 23 mg of reagent **4** were used on a 1:16 ratio between **4** and **2**, with 25 equivalents of the Lewis acid catalyst ($BF_3.Et_2O$). These conditions were inspired both by literature data and our laboratory preliminary investigations.[6,20] A preparative TLC was performed as purification step. Unfortunately, the desired copillar[4+1]arene could be

isolated with a yield lower than 1% (entry 1). The purification step was not adapted because of difficulties due to solubility issues, as explained in the next paragraph.

*Table 1 – Conditions and results obtained for copillar[4+1]arene **5** synthesis*

Entry	Mass of **4** (mg)	Eq. of $BF_3.Et_2O$	Ratio **4**:**2**	Yield (%)	Comments
1	23	25	1:16	< 1	Preparative TLC
2	23	25	1:16	2	One column[a]
3	52	25	1:16	/	One column
4	52	45	1:16	/	One column
5	52	25	1:16	10	Two columns
6	52	25	1:16	9	Two columns
7	52	39	1:16	9	Two columns
8	52	39	1:16	16	One column
9	**52**	**39**	**1:8**	**30**	**One column**
10	52	45	1:8	29	One column
11	200	39	1:8	/	One column
12	100	39	1:8	9	One column

a - The term "column" refers to the separation of the products by standard silica gel chromatography (see experimental part for conditions)

For attempt 2, it was decided to change the purification method, while using the same parameters as in entry 1. Column chromatography on silica gel was performed instead of the preparative TLC, but led to 2% yield (entry 2). The low yields obtained can be explained by two hypotheses. First, some solubility issues were encountered with the crude mixture, leading to purification difficulties. Those issues are probably caused by the presence of polymers, known as one of the by product's copillar[4+1]arene synthesis.[34] Indeed, the excess of **2** can react to form either pillar[5]arene, or polymers. Second, the scale used for the copillar[4+1]arene **5** synthesis is probably too low for the synthesis. In fact, as the copillar[4+1]arene **5** is the minor product, it is difficult to purify it with a large excess of pillar[5]arene and polymers. It was thus decided to increase the quantity of **4** engaged in the reaction from 23 mg to 52 mg (entry 3). However, the desired copillar[4+1]arene **20** could not be isolated, even if some traces of copillar[4+1]arene were seen in the crude NMR. The equivalent number of boron trifluoride diethyl etherate used is maybe not sufficient to achieve the synthesis, which could explain why the quantity of copillar[4+1]arene is so low. Indeed, as $BF_3.Et_2O$ increases the electrophilicity of paraformaldehyde, allowing the synthesis of methylene bridges of the copillar[4+1]arene, this Lewis acid catalyst must be added in a sufficient amount. Therefore, the equivalent number of boron trifluoride diethyl etherate was

increased from 25 to 45 equivalents (entry 4). Unfortunately, the desired copillar[4+1]arene **20** could not be isolated. Although copillar[4+1]arene **20** was clearly formed, no chromatographic fraction was pure. It was thus decided to perform two column chromatographies on silica gel as the purification step, using the same reagents conditions as entry 3. The desired copillar[4+1]arene **5** could be isolated with 10% yield (entry 5). This result could be reproduced a second time (entry 6). From those attempts, it can be concluded that two flash chromatographies have to be performed to isolate molecule **5**. As impurities remained in the product harvested after one flash chromatography, a second one must be performed to remove these impurities from the copillar[4+1]arene **5**. With those promising results in hands, it was decided to test again the influence of boron trifluoride diethyl etherate on the synthesis. The equivalent number of $BF_3.Et_2O$ was increased from 25 to 39 equivalents (entry 7). Unfortunately, attempt 7 gave the same 9% yield than attempts 5 and 6. The problems encountered are related to purification issues and not to reactivity. In fact, retention factors of all molecules (copillar[4+1]arene, pillar[5]arene and polymers) in the crude are so close, which make the purification step complicated. Thanks to the advice of our predecessor (Dr. W. Chen), the quantity of silica gel must be significantly increased, to make the purification step easier. In attempt 8, the same parameters as the entry 7 were used, while increasing the quantity of silica gel during the purification step by one flash chromatography (entry 8). Consequently, attempt 8 gave the desired copillar[4+1]arene **5** with 16% yield. Those conditions enabled to purify more desired product **5**, as the loss of product due to a second flash chromatography is minimized. Based on another advice of Dr. W. Chen and on the literature, the ratio between reagents **4** and **2** can be decreased from 1:16 to 1:8.[48] Indeed, decreasing the amount of **2** should limit the formation of by-products (pillar[5]arene and polymers) and thus, improve the yield. However, the ratio between **2** and **4** cannot be stoichiometric as copillar[3+2]arene formation can occur and therefore increase the by-product quantity.[49] The decrease of the ratio between **4** and **2** from 1:16 to 1:8 enabled to obtain the desired copillar[4+1]arene **5** with a satisfying 30% yield (entry 9). Then, to further exploit the influence of $BF_3.Et_2O$ number of equivalents on the copillar[4+1]arene synthesis, it was increased from 39 to 45 equivalents (entry 10). However, the yield was the same (29%). Indeed, once all reagent **4** (limiting reagent) has been already consumed, catalysis of the reaction is no longer useful as no more copillar[4+1]arene **5** can be synthetized. There will only be synthesis of by-products (pillar[5]arene and polymers), due to the excess of 2.

With the yield improvement from 1% to 30%, the reaction was further scaled up, from 52 to 200 mg of product **4** in the same conditions as entry 9 (entry 11). Unfortunately, at this reaction scale, the desired copillar[4+1]arene **5** could not be isolated. Perhaps the scale up should be done step by step and not directly from 52 mg to 200 mg of **4**. So, next attempt was performed on a 100 mg scale, using the same conditions as entry 9. This allows the synthesis of desired molecule **5** with 9% (entry 12). It can be concluded from these last attempts (entry 11 and 12) that scaling up the synthesis does not seem to be easy, as the thermodynamic of the reaction seems different at a larger scale.

III.2 Synthesis of 9OAc-SA

The copillar[4+1]arene **5** now synthetized, the focus was on the synthesis of sialic acid derivatives (Scheme 4). The synthesis of the final product **13** (9OAc-SA) can be achieved thanks to a multi-step pathway. The first reaction, leading to the synthesis of carbohydrate **7**, was achieved with a quantitative 99% yield on a multigram scale. The commercial starting material **6** was engaged in an esterification reaction in presence of Dowex®50WX2 (H^+) in dry methanol.[50] Then, peracetylation on a multigram scale was achieved by reaction of compound **7** with acetic anhydride in pyridine, catalysed by DMAP and gave 84% yield. A α/β mixture (14/86, as determined by ^{1}H NMR) was obtained, after a purification step by flash chromatography. The next step gave the intermediate chloride **9** with 84% yield, by treating the peracetylated molecule **8** with acetyl chloride, in a mixture of methanol and dichloromethane, on a multigram scale. A purification step was also needed for this reaction, taking care to separate the two diasteroisomers to only keep the β one.[51] In fact, the final clickable derivative **13** needs to be α configured and as the following propargylation reaction normally inverts the configuration, it is necessary to isolate the β diasteroisomer of intermediate chloride (**9b**).[5,21] Indeed, the mechanism of molecule **9** synthesis is likely a S_N1, due to the polar and acidic nature of the reaction medium. The purification of **9** led to a α/βmixture (greater than 5/95, as determined by ^{1}H NMR). However, molecule **9b** (the β anomer of **9**) was successfully isolated after a second flash chromatography, on a 200 mg batch.

Molecules **7**, **8**, and **9** are known compounds and their characterization and configuration assignments is based on literature data.[50–52]

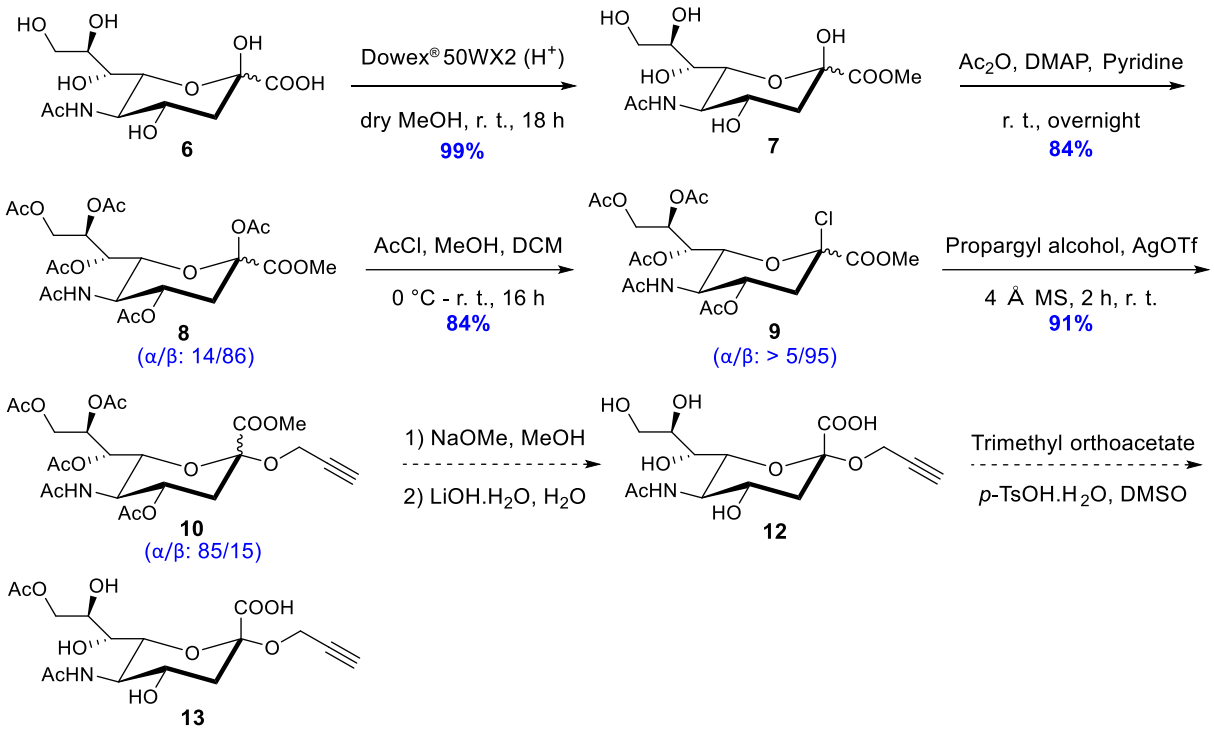

Scheme 4 - Synthetic pathway of the sialic acid derivatives

The synthesis of the α diastereoisomer of **10** by treating the intermediate chloride **9** with propargyl alcohol catalysed by silver triflate was then attempted on a 1 g scale. The first try was unsuccessful probably due to the degradation of commercial silver triflate used, by water. Indeed, distillation of propargyl alcohol is mandatory to avoid the degradation of the catalyst, silver triflate, by water. The reaction using freshly distilled propargyl alcohol then led to 91% yield. A α/β mixture (85/15, as determined by ^{1}H NMR) was obtained, after a purification step by column chromatography on silica gel. So, a second flash chromatography was performed, trying to separate the two diasteroisomers and only keep the α one. Unfortunately, this trial failed because of the co-elution of both diasteroisomers during flash chromatography.

To have a better understanding of the propargylation mechanism, a propargylation reaction was carried out on pure β anomer **9b** (200 mg) to see whether or not it would lead to a pure α diasteroisomer of **10** (**10a**). A α/β mixture (77/23, as determined by ^{1}H NMR) was still obtained, confirming that the glycosylation is not a pure S_N2 reaction. If the propargylation mechanism was a pure S_N2, there would have been a total inversion of configuration and would have resulted in molecule **10a**. Indeed, glycosylation reactions are mostly a S_N1/S_N2 continuum, meaning that these reactions can take place through a S_N1 and S_N2 mechanism simultaneously, which is either called S_N1-like or S_N2-like reactions.[53] In this case, the hypothesis of a S_N2-

like mechanism is most likely, as the mesomeric electron-withdrawing character of the methyl ester disfavours the S_N1 mechanism. Kinetic measurements should be performed to confirm this hypothesis.[54]

Because of the S_N2-like propargylation reaction, another way to purify carbohydrate **10** has to be performed. So, recrystallization conditions were attempted to separate the α diasteroisomer (**10a**) from the β one (**10b**).[55] A methodological work has been done to optimize the separation. All conditions are summarized in Table 2.

*Table 2 – Conditions and results obtained for molecule **10** recrystallization*

Entry	m (g)	Solvent	V (mL)	Work-up	Condition	α/β ratio[a, b]	α/β ratio[a, c]	Yield (%)
1	0,10	EtOH	3,0	Filtration	-20 °C	84/16	84/16	/
2	0,75	EtOH	3,0	Filtration	-20 °C	84/16	84/16	/
3	0,75	EtOH	1,0	Centrifugation	-20 °C	84/16	84/16	1
4	1,50	EtOH	4,0	Centrifugation	r. t.	85/15	85/15	< 1
5	2,50	EtOH	1,5	Centrifugation	r. t.	84/16	Degradation	< 1
6	1,00	Et_2O MeOH	5,0 3,6	Centrifugation	r. t.	85/15	85/15	2
7	0,50	Et_2O MeOH	2,5 0,90	/	r. t. to 4 °C to -20 °C	85/15	85/15	/
8	0,50	Et_2O MeOH	2,5 0,40	Centrifugation	r. t.	85/15	95/5	27
9	0,75	Et_2O MeOH	3,7 0,60	Centrifugation	r. t.	85/15	95/5	26
10	**0,30**[d]	**Et_2O MeOH**	**1,5 0,24**	**Centrifugation**	**r. t.**	**95/5**	**97/3**	**71**

a - All α/β ratios are quantified by ^{1}H NMR
b - α/β ratios of molecule **10** before recrystallization
c - α/β ratios of molecule **10** after recrystallization
d - The 300 mg are composed of enriched product (α/β: 95/5) harvested of entry 8 and 9. This is a second recrystallization to further purify product **10**.

The first recrystallization attempts were performed in ethanol.[56] For the first attempt, recrystallization has been tested on 100 mg scale, with 3 mL of ethanol (entry 1). Unfortunately, the small amount of product used for this recrystallization did not allow to obtain an efficient precipitation. The next experiment was attempted on a larger scale (750 mg), while using the same volume of ethanol (3.0 mL). Unfortunately, the fine powder observed as a suspension passed through the fritted glass filter (entry 2). Centrifugation was therefore chosen for the next experiments. In entry 3, the quantity of ethanol was reduced to 1.0 mL, using the same mass of product as entry 2. The 10 mg of solid obtained after centrifugation exhibits the same α/β ratio as in the starting material. In order to have a pure α molecule, the conditions were changed,

letting now to room temperature exclusively. Attempt 4 gave the same results as before. Attempt 5 led to product degradation as not enough solvent was added during the heating.

The recrystallization solvent was then changed, in accordance with the literature.[55] Diethyl ether was used as non-solvent and methanol as solvent. Attempt 6 was performed on a 1.00 g scale, using 5.0 mL of Et_2O and 3.6 mL of MeOH added progressively while heating. The result was the same as too much MeOH was added. The desired product and the impurities were therefore both solubilized at room temperature (before heating) in the solvent, making the separation difficult. The first parameter changed was the temperature, going from room temperature through 4 °C to -20 °C (entry 7). However, no crystals were observed. The second parameter changed was the volume of co-solvent added. We further decreased the quantity of methanol to 0.4 mL with 2.5 mL of diethyl ether, on a 500 mg scale. After being left at room temperature over week-end (70 h), crystals were formed. Product **10** was obtained (134 mg) and the ratio was changed from 85/15 to 95/5 (entry 8). This result was reproduced a second time, on a 750 mg scale (entry 9). Then, a second recrystallization was attempted on 300 mg, composed of enriched product (α/β: 95/5, as determined by ^{1}H NMR) harvested of entry 8 and 9 (entry 10). This second recrystallization, using the same conditions as entry 8 and 9, allowed to further purify product **10** (α/β: 97/3, as determined by ^{1}H NMR).

We are aware that ^{1}H NMR is not the most suited analytical technique to precisely quantify impurities present in less than 5%. However, the results described in entries 8-10 signify that the use of the dual solvents system Et_2O:MeOH can lead to significant enrichment in the desired α anomer which is still contaminated by, rougly, 3% of the β anomer. This level of purity is still not sufficient to go further in the preparation of molecules amenable to biological assays, but these results are more than encouraging.

In parallel of the recrystallization assays, the next steps achieving the synthesis of 9OAc-SA were tested with a α/β mixture (79/21, as determined by ^{1}H NMR) of **10**. Molecule **12** was successfully synthetized, in α/β mixture (82/18, as determined by ^{1}H NMR), with 90% yield (see Scheme 4, above). The synthesis was carried out in two deprotection steps. The first was the treatment of the acetates by methanol and sodium methoxide to give the resulting alcohols, by the so-called Zemplén reaction. The second was the deprotection of methyl ester with lithium hydroxide monohydrate in water, to give the resulting carboxylic acid. Finally, one more step needs to be performed to finally achieve the synthesis of clickable derivative **13**.

IV. Conclusions

Thanks to a methodology study, copillar[4+1]arene **5** has been successfully synthesized and the yield was improved from 2% to 30%, for a 50 mg scale. The global amount of copillar[4+1]arene **5** obtained to date is 130 mg. Firstly, the issues encountered mostly arise from the purification step due to the close retention factors of the different molecules generated and because the desired product is not the major one. Furthermore, boron trifluoride diethyl etherate ($BF_3.Et_2O$) should be added in sufficient amount which is 39 equivalents. Then, the ratio's best compromise between the two units, **2** and **4**, contained in the copillar[4+1]arene **5**, is 1 equivalent of **4** for 8 equivalents of **2** (Scheme 5).

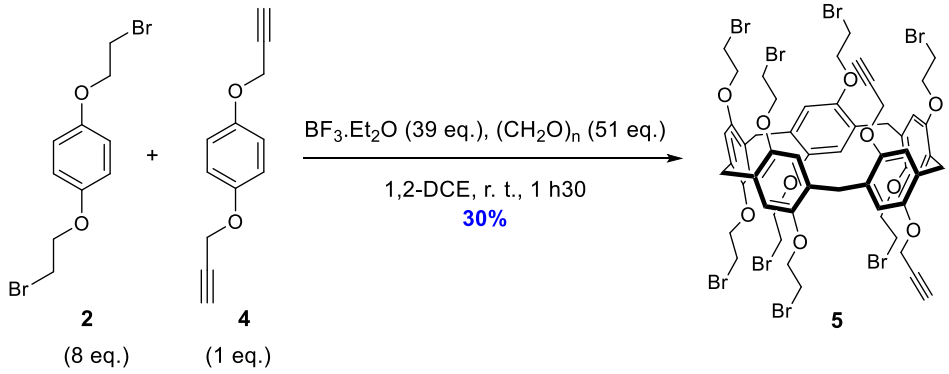

*Scheme 5 – Optimized synthetic pathway of the copillar[4+1]arene **5***

Concerning the sialic acid derivatives, clickable derivative **13** synthesis is already well underway (Scheme 6). The first reaction, leading to the synthesis of carbohydrate **7**, was achieved with a quantitative 99% yield. Then, molecule **8** synthesis gave 84% yield, with a α/β mixture (14/86, as determined by ^{1}H NMR). The intermediate chloride **9** and molecule **10** were synthetized with good yields of respectively 84 and 91%, with α/β mixtures greater than 5/95 and of 85/15. The propargylation reaction, leading to molecule **10** is a crucial step as the separation of the two diasteroisomers has to be performed here. Recrystallization is mandatory as the diasteroisomers cannot be separated by flash chromatography due to co-spotting. An optimization of this purification led us to various conclusions. Recrystallization in ethanol did not work in our hands, as only a suspension was obtained. The best recrystallization conditions are therefore 2.5 mL of diethyl ether as non-solvent and 0.4 mL of methanol as solvent on a 500 mg scale. Enrichment was obtained, over week-end (70 h) at room temperature, increasing the α/β ratio from 85/15 to 95/5. A second recrystallization of this enriched product further allow the purification of product **10** (α/β: 97/3). Next, to better understand the mechanism of propargylation reaction, a glycosylation has been carried out with a β diasteroisomer of intermediate chloride **9**. As a α/β mixture (77/23, as determined by ^{1}H NMR) was still obtained,

this showed that the mechanism is not a S_N2, it is probably a S_N2-like. Indeed, it is explained in the literature that glycosylations are most of the time a S_N1/S_N2 continuum.[53]

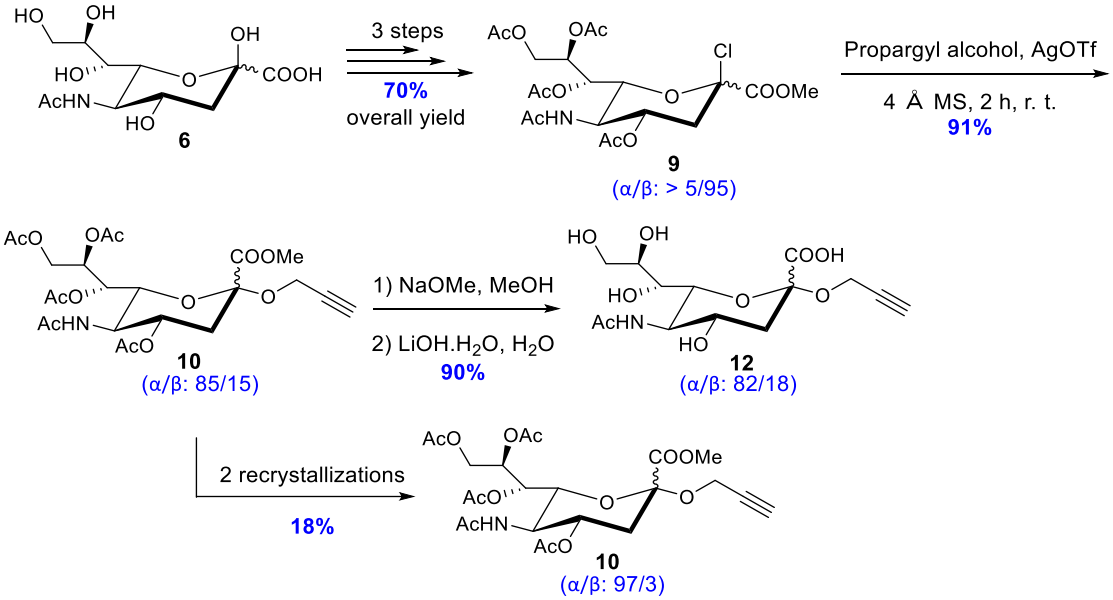

Scheme 6 – Summary of the sialic acid derivatives already synthetized

The two following deprotection steps of the 9OAc-SA multi-step synthesis were tested, although α/β mixtures were used as starting materials. These reactions gave promising results as product **12** was successfully synthetized, despite the presence of impurities, with an α/β mixture (82/18, as determined by ^{1}H NMR).

V. Outlooks

V.1 Synthesis of 9OAc-SA

On one hand, the multi-step pathway for the synthesis of the sialic acid derivative **13** should be achieved, once the α diasteroisomer of molecule **10** (**10a**) is obtained (Scheme 7). This will still require purification of molecule **10** by recrystallization, although promising results have already been obtained. Then, the two deprotection steps will have to be performed on molecule **10a**, to complete the synthesis of product **12**. Finally, a methodological work on the last step, achieving the synthesis of 9OAc-SA **13** will probably have to be carried out as monoacetylation must be selective to the 9-positon.[5] The most usual selective acetylation procedure relies on the protocol pioneered by Ogura which uses trimethyl orthoacetate under acidic catalysis.[57]

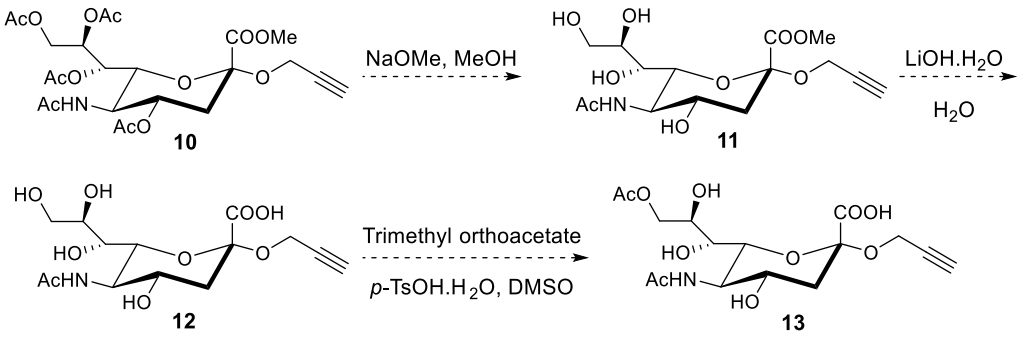

*Scheme 7 – Completion of the synthetic pathway of the sialic acid derivative **13***

V.2 Peptide synthesis

On the other hand, the peptide synthesis will have to be carried out (Scheme 8). To insert ACE2-derived peptide, a pentaglycine peptide will be first functionalized on the copillar[4+1]arene **5**. Then, it will be possible to carry out a sortase-mediated ligation reaction.

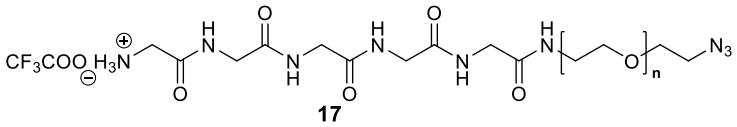

*Scheme 8 - Structure of preliminary pentaglycine peptide **17***

V.3 CuAAC reactions

Afterwards, both sialic acid derivative **13** and peptide **17** will be coupled on the copillar[4+1]arene **5** by copper-catalysed alkyne-azide cycloadditions (CuAAC). Three steps are needed to finally achieve the synthesis of the target copillar[4+1]arene **20** (Scheme 9). This

is essential to avoid having both alkynes and azides simultaneously on the scaffold, due to the possible polymerisation between them. This is why peptide **17** is first coupled to the copillar[4+1]arene **5**, by CuAAC. Then, an azidation reaction is carried out to enable the second click reaction between copillar[4+1]arene **19** and 9OAc-SA **13**.

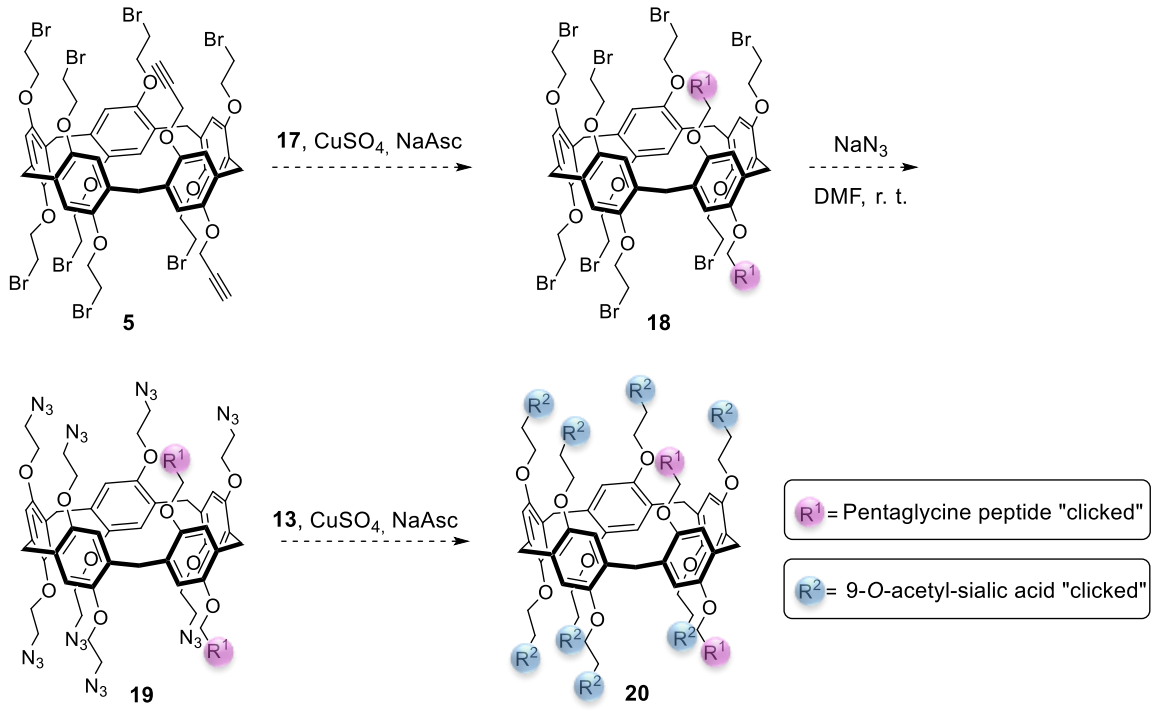

*Scheme 9 - Synthetic pathway of final copillar[4+1]arene **20***

VI. Experimental part

VI.1 General information

Reagents and chemicals were purchased from Merk-Sigma-Aldrich or Acros at ACS grade and were used without purification if not stated. Propargyl alcohol was distilled before used. The distillation was carried out under pressure, at 180 mbar and 80°C, in the presence of pumice stones and K_2CO_3. Dry acetonitrile, acetone and methanol used as reaction solvents were purchased with an AcroSeal packaging.

All reactions were monitored by thin-layer chromatography (TLC) carried out on Merck aluminium sheets silica gel 60-F_{254}, using UV light (fluorescence quenching detection at 254 nm) and/or a potassium permanganate solution as TLC stain. Retention factors (R_F) are indicated with the corresponding eluent used.

All column chromatographies were performed on Roth silica gel 60, 0.040-0.063 nm (400-230 mesh). The indicated solvents mixture ratios are given in volume fractions.

The NMR spectra used for the characterization of all the synthetized molecules were recorded either on a JEOL ECX-400 (at 400 MHz for ^{1}H and 101 MHz for ^{13}C) or on a JEOL ECZ-500R (at 500 MHz for ^{1}H and 126 MHz for ^{13}C). All compounds were characterized by ^{1}H and ^{13}C NMR. The abbreviations used to define the multiplicities are, s= singlet, d= doublet, t= triplet, q= quadruplet, m= multiplet, dd= doublet of doublets, ddd= doublet of doublet of doublets, td= triplet of doublets, dtd= doublet of triplet of doublets. Chemical shifts (δ) are reported in ppm and referenced indirectly to residual solvent signals. ($CDCl_3$: ^{1}H 7.26 ppm, ^{13}C 77.16 ppm, CD_3OD: ^{1}H 3.31 ppm, ^{13}C 49.00 ppm). All the spectra were realized in $CDCl_3$ or CD_3OD.

Melting points were determined in capillary tubes with a Büchi M-560 melting points instruments.

VI.2 Syntheses and protocols

VI.2.1 Synthesis of 1,4-bis(2-bromoethoxy)benzene (**2**):

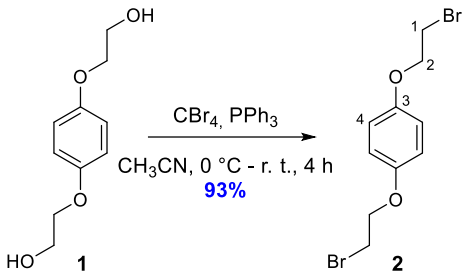

To a solution of 1,4-bis(2-hydroxyethoxy)benzene **1** (4.01 g, 20.23 mmol, 1 eq.) and PPh_3 (11.65 g, 44.42 mmol, 2.2 eq.) in dry acetonitrile (80 mL) was slowly added CBr_4 (14.73 g, 44.42 mmol, 2.2 eq.). The mixture was vigorously stirred under argon atmosphere at 0 °C for 10 min. After stirring for 4 h at room temperature, H_2O (60 mL) was added to the reaction mixture. The mixture was filtered and the crude was washed with methanol/water mixture (90 mL/60 mL) to give the desired product **2** as a white amorphous powder (6.08 g, 18.76 mmol, 93%).

- **Chemical Formula**: $C_{10}H_{12}Br_2O_2$
- **Molecular weight**: 324.01 g/mol
- **Aspect**: white amorphous powder
- **R_F**: 0.6 (EtOAc/Cyclohexane: 1/1)
- **^{1}H NMR (500 MHz, $CDCl_3$)** δ (ppm): 6.86 (s, 4H, H-4), 4.24 (t, *J*= 6.3 Hz, 4H, H-2), 3.62 (t, *J*= 6.3 Hz, 4H, H-1).
- **^{13}C NMR (126 MHz, $CDCl_3$)** δ (ppm): 152.9, 116.2, 68.8, 29.4.

NMR analyses are in agreement with literature.[58]

^{1}H NMR spectrum of compound 2 recorded in $CDCl_3$ at 500 MHz

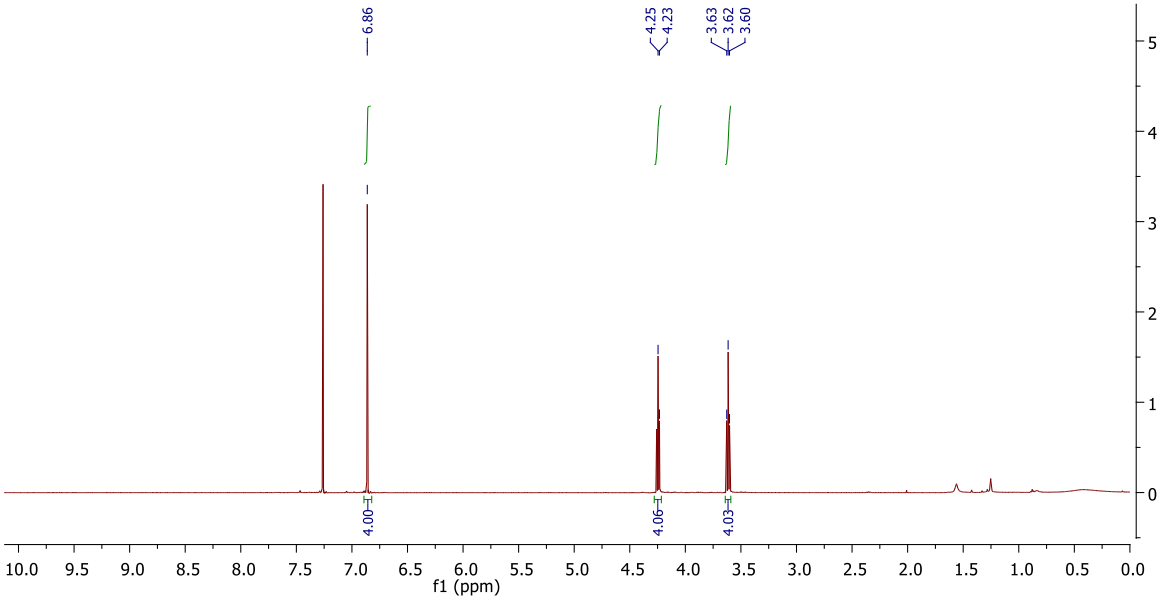

^{13}C NMR spectrum of compound 2 recorded in $CDCl_3$ at 126 MHz

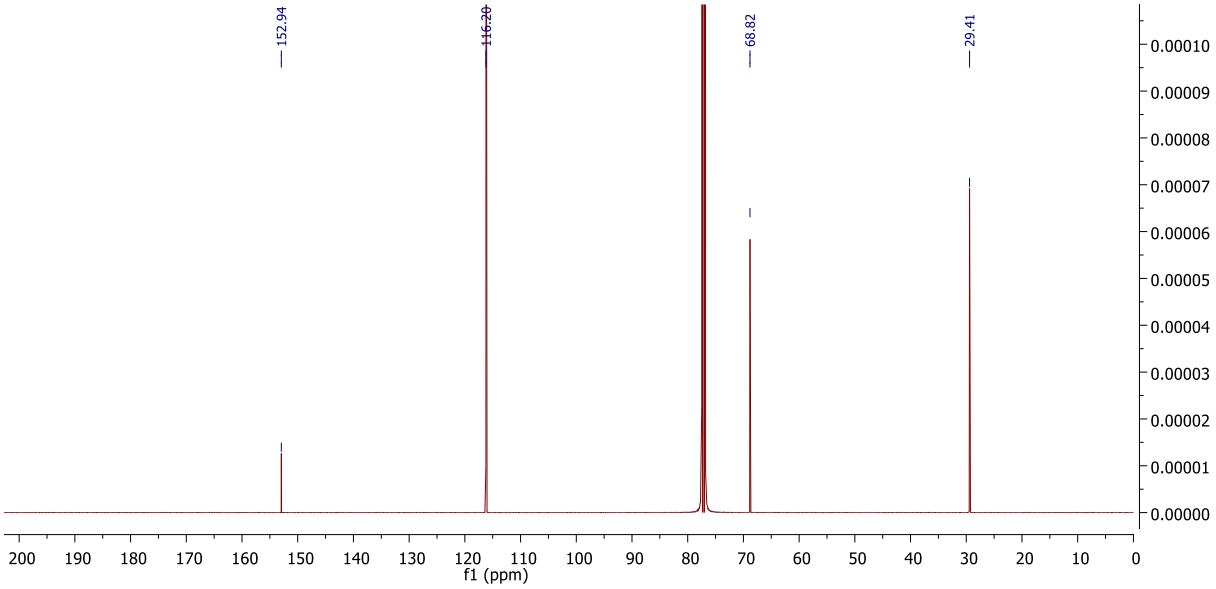

VI.2.2 Synthesis of 1,4-bis(2-propargyloxy)benzene (**4**):

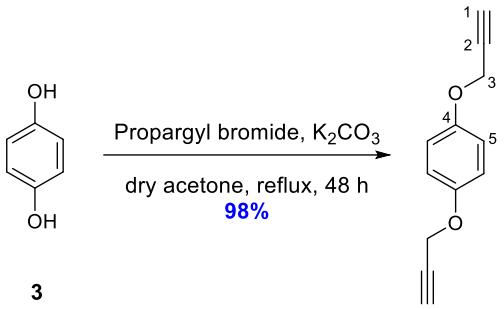

3 **4**

To a solution of hydroquinone **3** (4.01 g, 36.42 mmol, 1 eq.) in dry acetone (91 mL) was added K_2CO_3 (25.12 g, 181.8 mmol, 5 eq.) under argon atmosphere. The reaction mixture was refluxed for 30 min. Then, propargyl bromide 80% (12 mL, 111 mmol, 3 eq.) was added dropwise and the reaction mixture was refluxed for 48 h before cooling down, followed by filtration. The filtrate was then evaporated, giving a brown solid (6.61 g, 35.50 mmol, 98%).

- **Chemical Formula**: $C_{12}H_{10}O_2$
- **Molecular weight**: 186.21 g/mol
- **Aspect**: brown solid
- **R_F**: 0.6 (EtOAc/Cyclohexane: 1/1)
- **^{1}H NMR (500 MHz, $CDCl_3$)** δ (ppm): 6.93 (s, 4H, H-5), 4.65 (d, *J*= 2.4 Hz, 4H, H-3), 2.51 (t, *J*= 2.4 Hz, 2H, H-1).
- **^{13}C NMR (101 MHz, $CDCl_3$)** δ (ppm): 152.5, 116.2, 78.9, 75.5, 56.6.

NMR analyses are in agreement with literature.[59]

^{1}H NMR spectrum of compound 4 recorded in $CDCl_3$ at 500 MHz

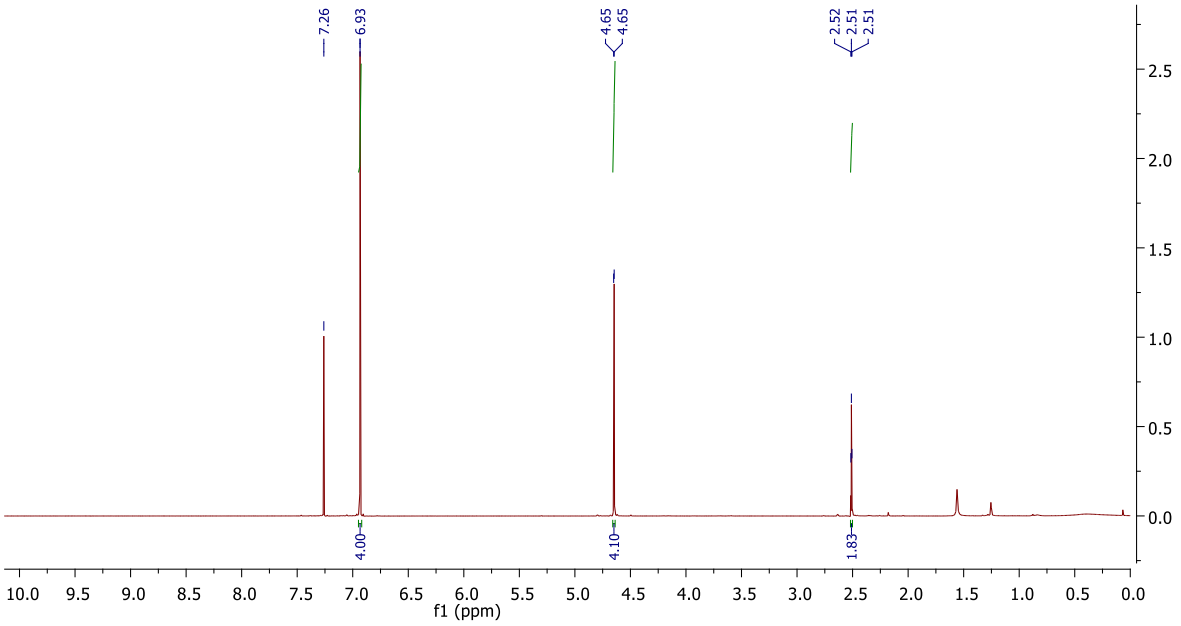

^{13}C NMR spectrum of compound 4 recorded in $CDCl_3$ at 101 MHz

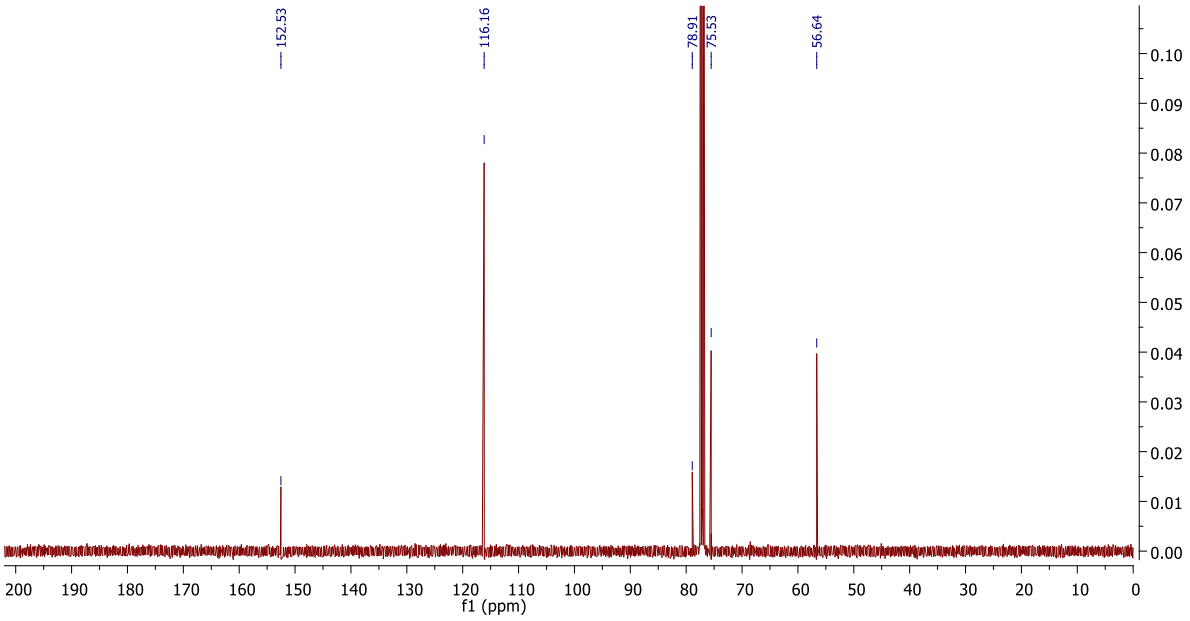

VI.2.3 Synthesis of copillar[4+1]arene (**5**):

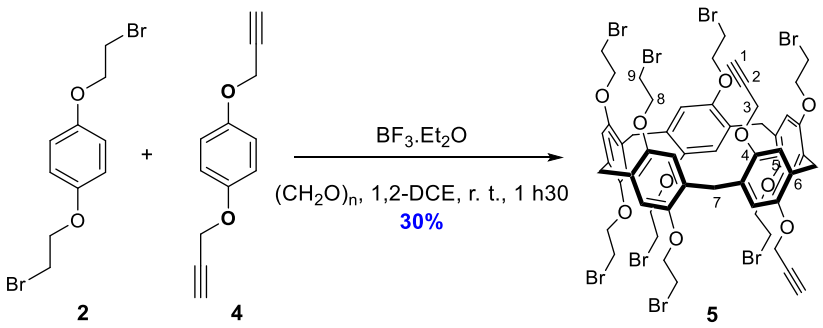

To a mixture of 1,4-bis(2-propargyloxy)benzene **4** (52 mg, 0.277 mmol, 1 eq.), 1,4-bis(2-bromoethoxy)benzene **2** (697 mg, 2.15 mmol, 8 eq.) and paraformaldehyde (427 mg, 14.2 mmol, 51 eq.) was added 1,2-DCE (34.5 mL) under argon atmosphere. Then, $BF_3.Et_2O$ (1.3 mL, 10.53 mmol, 39 eq.) was added dropwise to the reaction mixture. After stirring for 1 h30 at room temperature, the reaction was quenched by addition of MeOH (30 mL) before being concentrated under vacuum. Afterwards, DCM (25 mL) was added to the residue before filtrating. The filtrate was then concentrated under vacuum and the crude was purified by column chromatography on silica gel using DCM/Cyclohexane 50/50 as eluent, under isocratic conditions. The desired compound **5** was isolated as a white solid (130.3 mg, 0.084 mmol, 30% yield).

- **Chemical Formula**: $C_{57}H_{58}Br_8O_{10}$
- **Molecular weight**: 1542.31 g/mol
- **Aspect**: white solid
- **R_F**: 0.1 (DCM/Cyclohexane: 1/1)
- **^{1}H NMR (500 MHz, $CDCl_3$)** δ (ppm): 6.91 (s, 2H, H-5), 6.87 – 6.86 (m, 6H, H-5), 6.76 (s, 2H, H-5), 4.58 (d, *J*= 2.3 Hz, 4H, H-3), 4.23 – 4.13 (m, 16H, H-8), 3.85 – 3.83 (m, 10H, H-7), 3.60 (dtd, *J*= 26.3, 5.6, 3.2 Hz, 16H, H-9), 2.20 (t, *J*= 2.3 Hz, 2H, H-1).
- **^{13}C NMR (126 MHz, $CDCl_3$)** δ (ppm): 149.9, 149.8, 149.8, 149.4, 129.5, 129.2, 129.1, 129.0, 116.3, 116.3, 116.0, 115.9, 115.8, 79.3, 75.0, 69.2, 69.2, 69.0, 68.9, 56.7, 30.8, 30.7, 30.5, 29.9, 29.8, 29.5, 29.5.

NMR analyses are in agreement with literature.[6]

^{1}H NMR spectrum of compound 5 recorded in $CDCl_3$ at 500 MHz

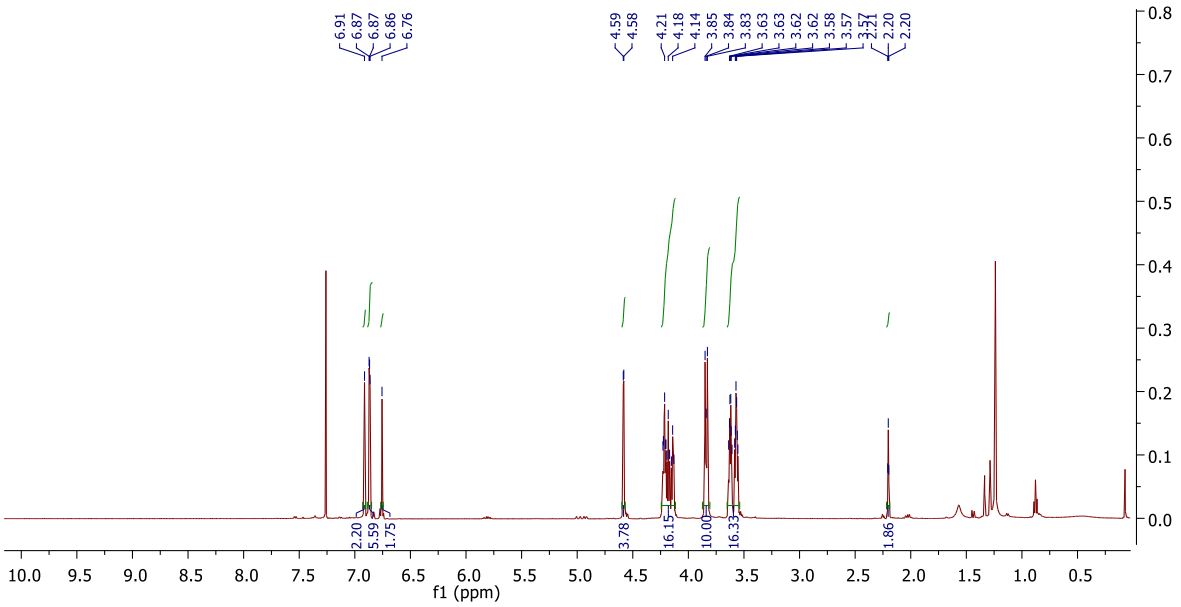

^{13}C NMR spectrum of compound 5 recorded in $CDCl_3$ at 126 MHz

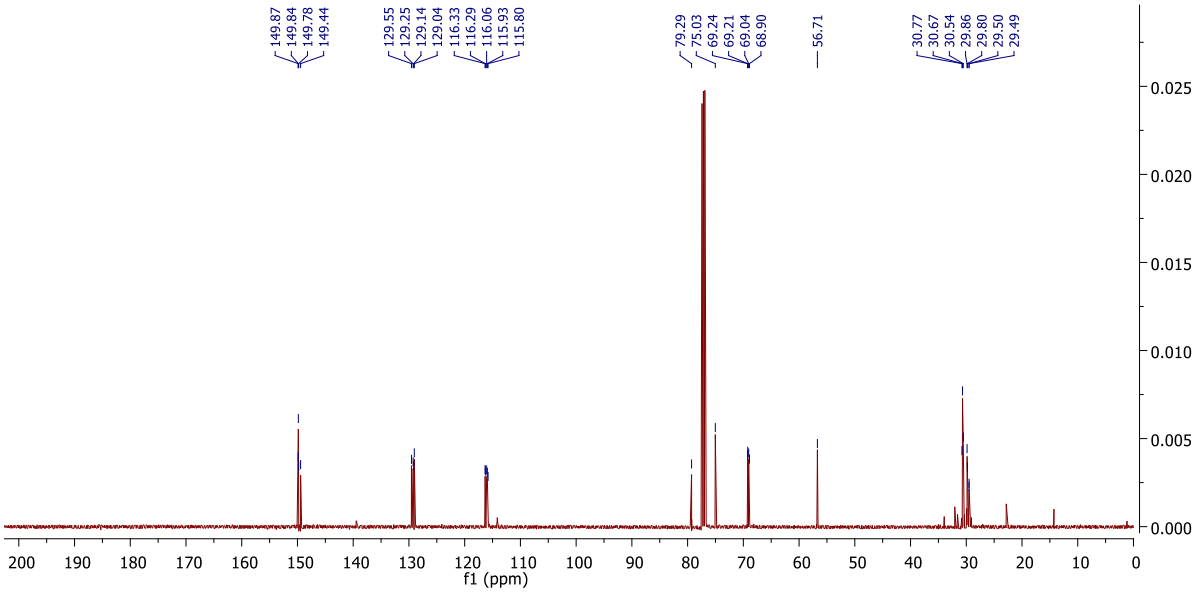

VI.2.4 Synthesis of *N*-acetyl-neuraminic acid methyl ester (**7**):

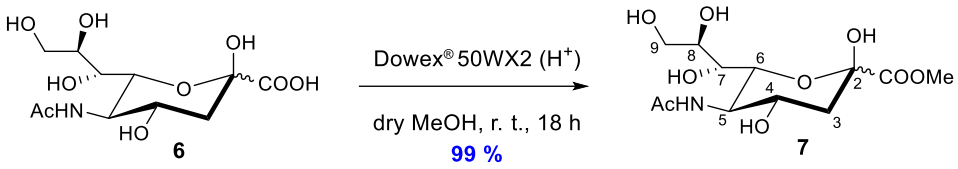

To a solution of *N*-acetyl neuraminic acid **6** (4.04 g, 13.06 mmol, 1 eq.) in dry MeOH (150 mL) was added Dowex®50WX2 (H^+, 2.03 g) under argon atmosphere. The reaction mixture was stirred for 18 h at room temperature. The resin was then filtered and washed with MeOH (25 mL). Finally, the filtrate was evaporated under vacuum to obtain a white solid (4.18 g, 12.93 mmol, 99% yield).

- **Chemical Formula**: $C_{12}H_{21}NO_9$
- **Molecular weight**: 323.30 g/mol
- **Aspect**: white solid
- **R_F**: 0.6 (MeOH/DCM: 3/7)
- **m. p**.: / (degradation point at 184 °C)
- **^{1}H NMR (500 MHz, CD_3OD)** δ (ppm): 8.17 (d, *J*= 8.7 Hz, 1H, NH), 4.06 – 3.98 (m, 2H, H-4, H-6), 3.84 – 3.78 (m, 2H, H-5, H-9a), 3.78 (s, 3H, CO_2CH_3), 3.72 – 3.68 (m, 1H, H-8), 3.62 (dd, *J*= 11.3, 5.7 Hz, 1H, H-9b), 3.48 (dd, *J*= 9.2, 1.4 Hz, 1H, H-7), 2.21 (dd, *J*= 12.9, 4.9 Hz, 1H, H-3eq), 2.02 (s, 3H, NAc), 1.89 (dd, *J*= 12.8, 11.5 Hz, 1H, H-3ax).
- **^{13}C NMR (126 MHz, CD_3OD)** δ (ppm): 175.1, 171.8, 96.7, 72.1, 71.6, 70.2, 67.8, 64.8, 54.3, 53.1, 40.7, 22.6.

NMR analyses are in agreement with literature.[50]

^{1}H NMR spectrum of compound 7 recorded in CD_3OD at 500 MHz

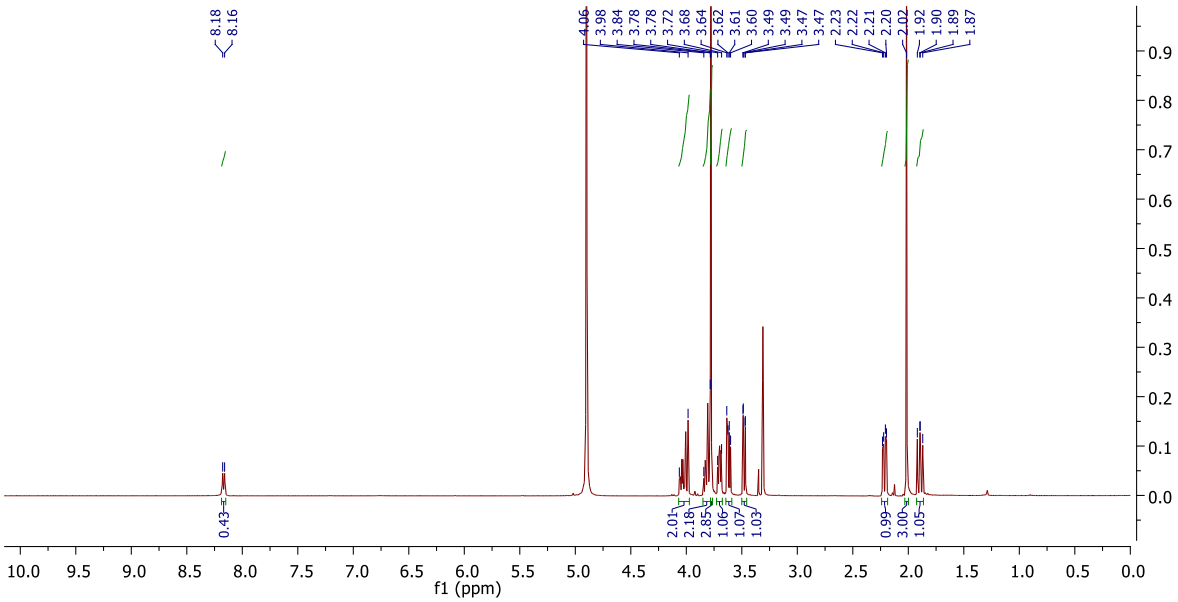

^{13}C NMR spectrum of compound 7 recorded in CD_3OD at 126 MHz

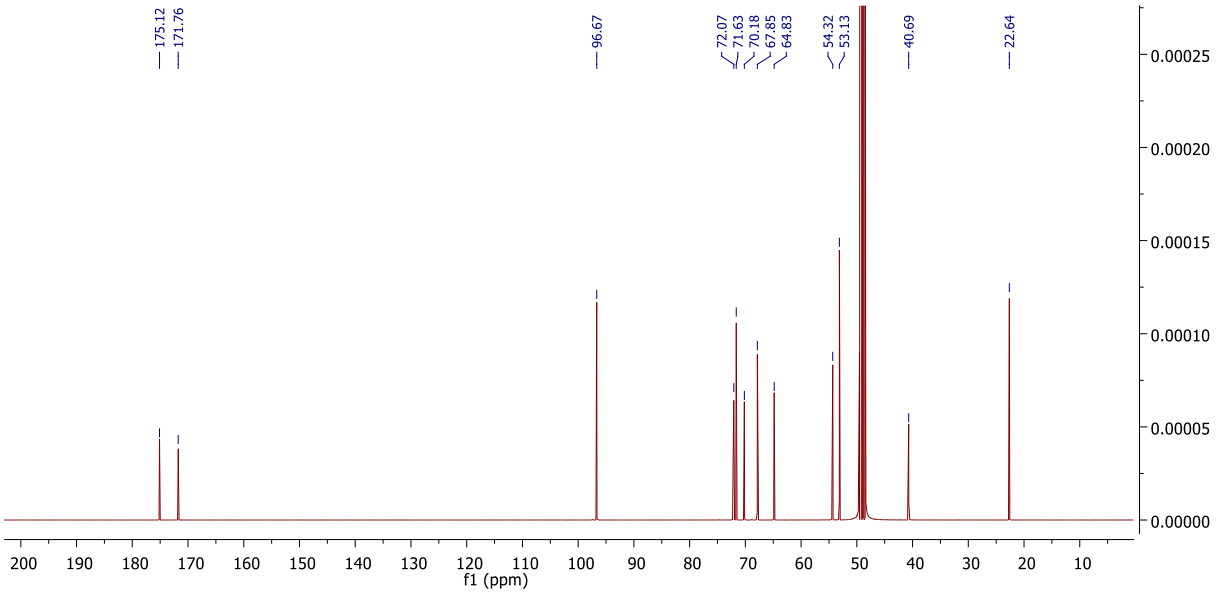

VI.2.5 Synthesis of *N*-acetyl-neuraminic acid methyl ester 2,4,7,8,9-pentaacetate (**8**):

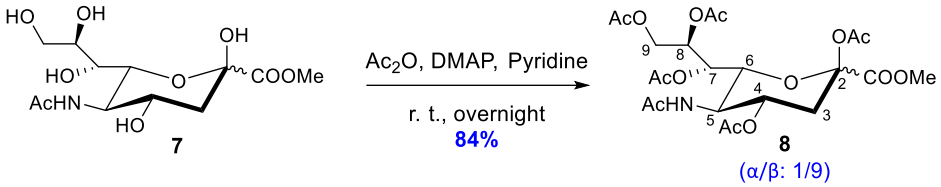

To a solution of white solid **7** (4.15 g, 12.84 mmol, 1 eq.) and DMAP (157 mg, 1.29 mmol, 0.1 eq.) in pyridine (50 mL) was slowly added Ac_2O (36 mL, 383 mmol, 30 eq.) at room temperature. After stirring overnight (16 h), the reaction mixture was concentrated under vacuum. The residue was dissolved in a minimum of DCM and the organic phase was washed respectively with 25 mL of HCl, water and brine. The organic phase was dried over $MgSO_4$, filtrated and concentrated under vacuum. The yellowish crude obtained was purified by column chromatography on silica gel using EtOAc/Cyclohexane as eluent from 70/30 to 100/0. The liquid deposit was done with DCM. The desired compound **8** was isolated as a white solid (5.76 g, 10.80 mmol, 84% yield, α/β mixture: 14/86[a]).

- **Chemical Formula**: $C_{22}H_{31}NO_{14}$
- **Molecular weight**: 533.48 g/mol
- **Aspect**: white solid
- **R_F**: 0.1 (EtOAc/Cyclohexane: 8/2)
- **m. p.**: 113 °C
- **^{1}H NMR (500 MHz, $CDCl_3$)** δ (ppm): 5.42 – 5.40 (m, 1H, NH), 5.37-5.35 (td, 1H, H-7), 5.26 – 5.21 (m, 1H, H-4), 5.05 (ddd, *J*= 6.8, 5.1, 2.6 Hz, 1H, H-8), 4.48 (dd, *J*= 12.4, 2.6 Hz, 1H, H-9a), 4.15 – 4.09 (m, 3H, H-5, H-6, H-9b), 3.78 (s, 3H, CO_2CH_3), 2.53 (dd, *J*= 13.4, 5.0 Hz, 1H, H3-ax), 2.13 – 2.02 (m, 16H, OAc), 1.88 (s, 3H, NAc).
- **^{13}C NMR (126 MHz, $CDCl_3$)** δ (ppm): 171.0, 170.6, 170.4, 170.3, 170.3, 168.3, 166.4, 97.5, 72.9, 71.5, 68.4, 67.8, 62.2, 53.2, 49.2, 36.0, 23.2, 21.0, 20.9, 20.8, 20.8, 20.8.

NMR analyses are in agreement with literature.[52]

[a]The α/β ratio is quantified by ^{1}H NMR.

^{1}H NMR spectrum of compound 8 recorded in $CDCl_3$ at 500 MHz

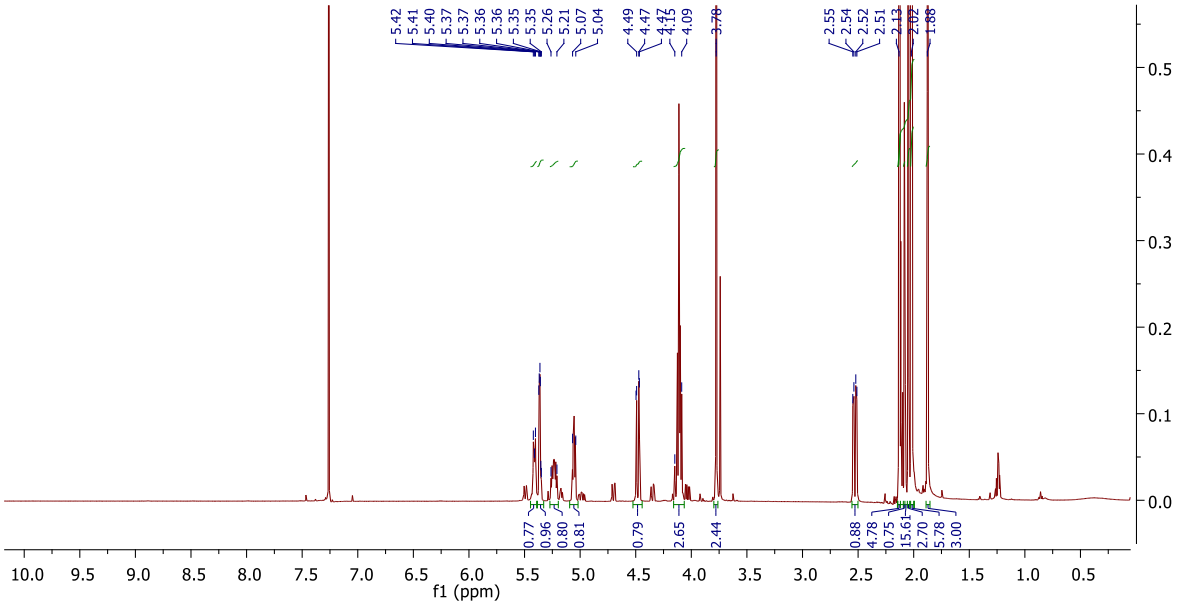

^{13}C NMR spectrum of compound 8 recorded in $CDCl_3$ at 126 MHz

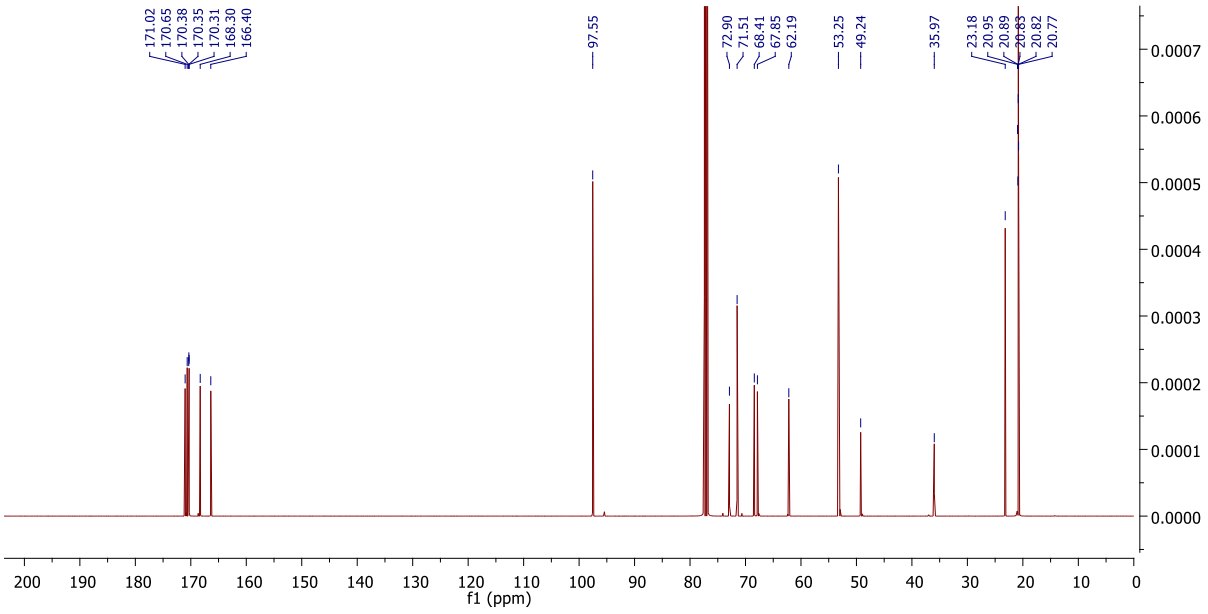

VI.2.6 Synthesis of *N*-acetyl-2-chloro-β-neuraminic acid methyl ester 4,7,8,9-tetraacetate (**9**):

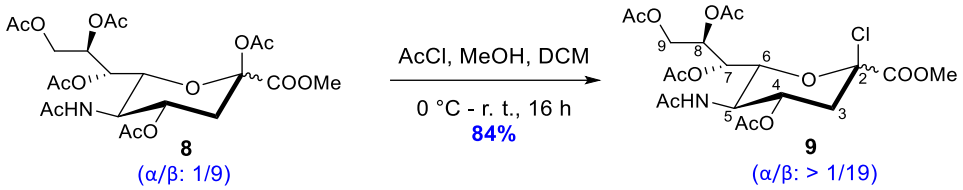

To a solution of **8** (4.11 g, 7.70 mmol, 1 eq.) in MeOH/DCM (5.4 mL/69 mL) was slowly added acetyl chloride (42 mL, 589 mmol, 76 eq.) under argon atmosphere at 0 °C and the mixture was stirred for 30 min. The mixture was then stirred for 16 h at room temperature before being concentrated under vacuum. The crude obtained was purified by column chromatography on silica gel using EtOAc/Cyclohexane as eluent from 80/20 to 100/0. The desired compound **9** was isolated as a white solid (3.31 g, 6.49 mmol, 84% yield, α/β mixture: > 5/95).

- **Chemical Formula**: $C_{20}H_{28}ClNO_{12}$
- **Molecular weight**: 509.89 g/mol
- **Aspect**: white solid
- **R_F**: 0.2 (EtOAc/Cyclohexane: 9/1[a])
- **m. p.**: 103 °C
- **^{1}H NMR (500 MHz, $CDCl_3$)** δ (ppm): 5.73 (d, *J*= 10.2 Hz, 1H, NH), 5.46 (dd, *J*= 6.7, 2.4 Hz, 1H, H-7), 5.38 (td, *J*= 11.0, 4.8 Hz, 1H, H-4), 5.15 (td, *J*= 6.2, 2.7 Hz, 1H, H-8), 4.42 (dd, *J*= 12.5, 2.7 Hz, 1H, H-9a), 4.35 (dd, *J*= 10.8, 2.4 Hz, 1H, H-5), 4.20 (q, *J*= 10.4 Hz, 1H, H-6), 4.05 (dd, *J*= 12.5, 6.1 Hz, 1H, H-9b), 3.85 (s, 3H, CO_2CH_3), 2.76 (dd, *J*= 13.9, 4.8 Hz, 1H, H-3eq), 2.25 (dd, *J*= 13.9, 11.2 Hz, 1H, H-3ax), 2.10 (s, 3H, OAc), 2.06 (s, 3H, OAc), 2.03 (s, 3H, OAc), 2.03 (s, 3H, OAc), 1.89 (s, 3H, NAc).
- **^{13}C NMR (101 MHz, $CDCl_3$)** δ (ppm): 170.9, 170.6, 170.6, 169.9, 165.6, 96.6, 73.9, 70.3, 68.8, 67.0, 62.1, 53.7, 48.4, 40.6, 23.0, 20.9, 20.8, 20.7.

[a]The α/β ratio is quantified by ^{1}H NMR.

A batch of **9** was taken to separate the two anomers and get 100 % of β anomer. Thus, a second column chromatography on silica gel using EtOAc/DCM as eluent from 50/50 to 60/40 was performed.

- **^{1}H NMR (500 MHz, $CDCl_3$)** δ (ppm): 5.47 (dd, *J*= 7.1, 2.4 Hz, 1H, H-7), 5.42-5.36 (m, 2H, H-4, NH), 5.17 (ddd, *J*= 7.1, 5.7, 2.7 Hz, 1H, H-8), 4.42 (dd, *J*= 12.5, 2.7 Hz, 1H, H-9a), 4.34 (dd, *J*= 10.8, 2.4 Hz, 1H, H-5), 4.21 (q, *J*= 10.4 Hz, 1H, H-6), 4.06 (dd, *J*= 12.6, 5.7 Hz, 1H, H-9b), 3.88 (s, 3H, CO_2CH_3), 2.78 (dd, *J*= 13.9, 4.8 Hz, 1H, H-3eq), 2.28 (dd, *J*= 13.9, 11.2 Hz, 1H, H-3ax), 2.12 (s, 3H, OAc), 2.08 (s, 3H, OAc), 2.06 (s, 3H, OAc), 2.05 (s, 3H, OAc), 1.91 (s, 3H, NAc).

NMR analyses are in agreement with literature.[51]

^{1}H NMR spectrum of compound 9 (α/β mixture) recorded in $CDCl_3$ at 500 MHz

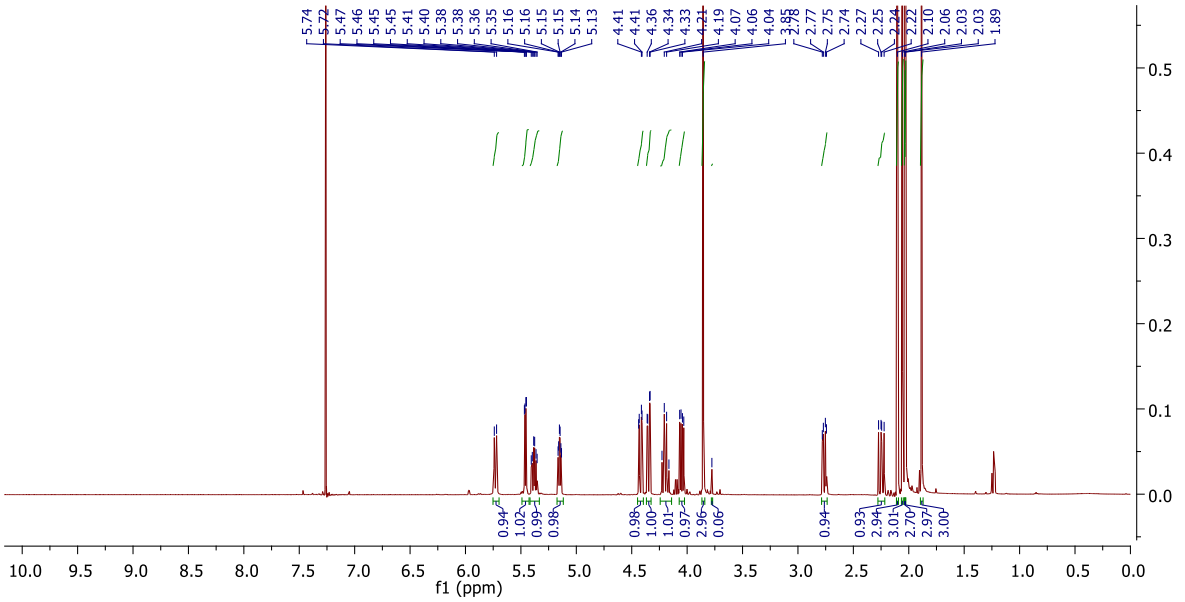

^{1}H NMR spectrum of compound 9 (β pure) recorded in $CDCl_3$ at 500 MHz

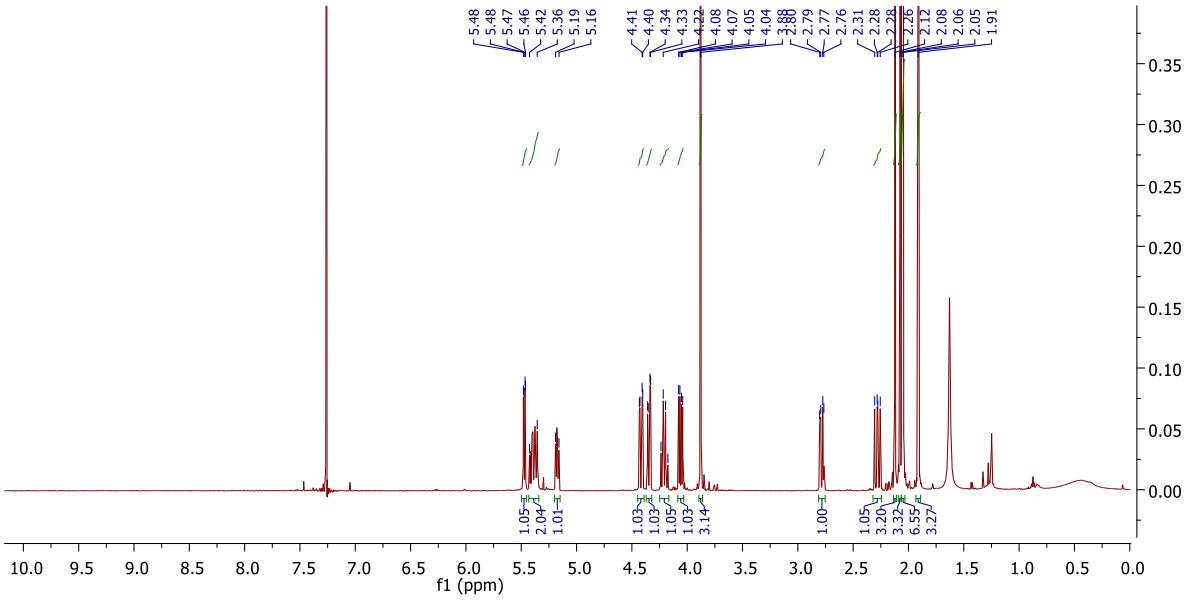

^{13}C NMR spectrum of compound 9 (α/β mixture) recorded in $CDCl_3$ at 101 MHz

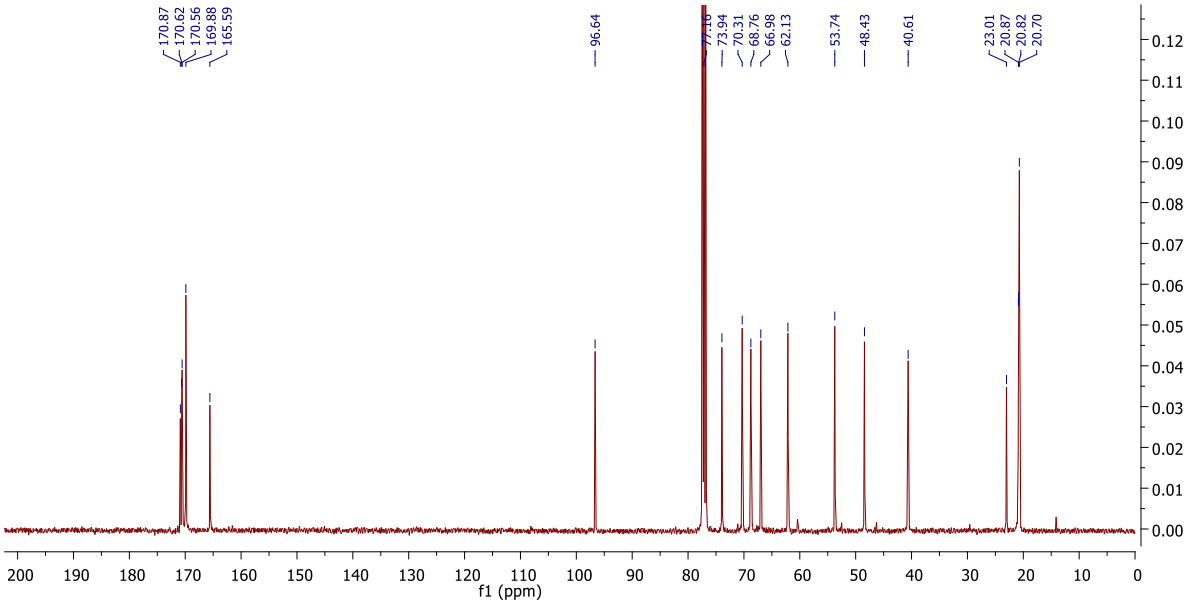

VI.2.7 Synthesis of *N*-acetyl-2-propargyl-α-neuraminic acid methyl ester 4,7,8,9-tetraacetate (**10**):

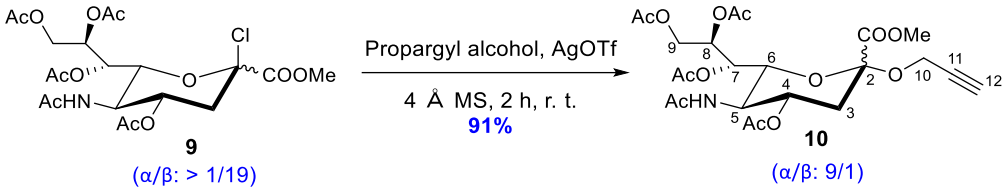

To a solution of **9** (1.00 g, 1.96 mmol, 1 eq.) and 4 Å molecular sieve (2 g) in freshly distilled propargyl alcohol (22 mL) was added silver triflate (756 mg, 2,94 mmol, 1.5 eq.) under argon atmosphere, at room temperature. The mixture was stirred for 2 h at room temperature before filtrating on cotton. The filtrate was then concentrated under vacuum and the crude obtained was purified by column chromatography on silica gel using EtOAc/Cyclohexane as eluent from 60/40 to 100/0. **10** was isolated as a white solid (947 mg, 1.79 mmol, 91% yield, α/β mixture: 85/15[a]).

- **Chemical Formula**: $C_{23}H_{31}NO_{13}$
- **Molecular weight**: 529.50 g/mol
- **Aspect**: white solid
- **R_F**: 0.3 (100 % EtOAc)
- **^{1}H NMR (500 MHz, $CDCl_3$)** δ (ppm): 5.43 – 5.40 (m, 1H, H-8), 5.31 (dd, *J*= 8.7, 1.6 Hz, 1H, H-7), 5.14 – 5.12 (m, 1H, NH), 4.87 (ddd, *J*= 12.3, 10.0, 4.6 Hz, 1H, H-4), 4.41 (dd, *J*= 15.7, 2.5 Hz, 1H, H-10a), 4.28 (dd, *J*= 12.4, 2.8 Hz, 1H, H-9a), 4.17 (dd, *J*= 15.7, 2.4 Hz, 1H, H-10b), 4.11 – 4.03 (m, 3H, H-5, H-6, H-9b), 3.82 (s, 3H, CO_2CH_3), 2.64 (dd, *J*= 12.8, 4.6 Hz, 1H, H-3eq), 2.44 (t, *J*= 2.5 Hz, 1H, H-12), 2.16 (s, 3H, OAc), 2.14 (s, 3H, OAc), 2.05 (s, 3H, OAc), 2.03 (s, 3H, OAc), 1.88 (s, 3H, NAc).

It is noteworthy that the resulting compound **10**, after two recrystallizations, still is a α/β mixture (97/3[a]), so only the ^{1}H NMR spectra are shown here.

- **^{1}H NMR (500 MHz, $CDCl_3$)** δ (ppm): 5.41 (ddd, J = 8.6, 5.7, 2.8 Hz, 1H, H-8), 5.31 (dd, J = 8.8, 1.6 Hz, 1H, H-7), 5.20 – 5.18 (m, 1H, NH), 4.87 (ddd, J = 12.3, 10.0, 4.7 Hz, 1H, H-4), 4.40 (dd, J = 15.7, 2.5 Hz, 1H, H-10a), 4.28 (dd, J = 12.4, 2.7 Hz, 1H, H-9a), 4.16 (dd, J = 15.7, 2.5 Hz, 1H, H-10b), 4.08 (dd, J = 12.3, 5.6 Hz, 3H, H-5, H-6, H-9b), 3.81 (s, 3H, CO_2CH_3), 2.63 (dd, J = 12.8, 4.6 Hz, 1H, H-3eq), 2.44 (t, J = 2.5 Hz, 1H, H-12), 2.16 (s, 3H, OAc), 2.14 (s, 3H, OAc), 2.04 (s, 3H, OAc), 2.03 (s, 3H, OAc), 1.88 (s, 3H, NAc).
- **^{13}C NMR (101 MHz, $CDCl_3$)** δ (ppm): 171.1, 170.8, 170.4, 170.3, 170.2, 167.9, 98.2, 79.1, 74.6, 72.7, 68.9, 68.3, 67.3, 62.5, 53.0, 53.0, 49.5, 38.0, 23.3, 21.3, 21.0, 21.0, 20.9.

[a]The α/β ratio is quantified by ^{1}H NMR.

NMR analyses are in agreement with literature.[60]

^{1}H NMR spectrum of compound 10, before recrystallization (α/β: 95/5) recorded in $CDCl_3$ at 500 MHz

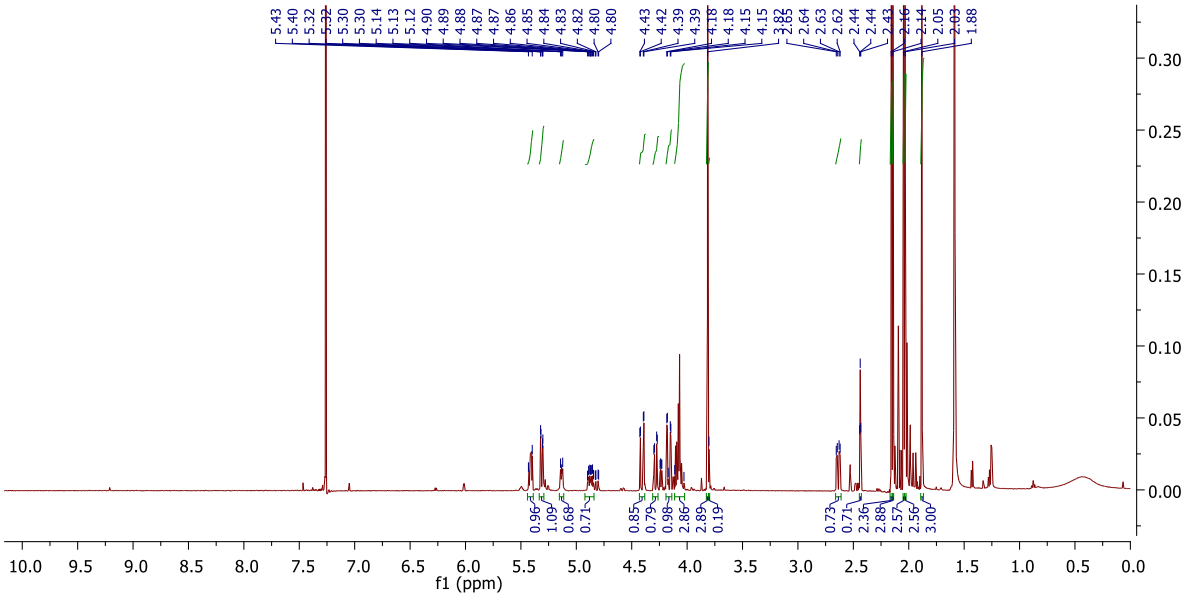

^{1}H NMR spectrum of compound 10, after recrystallization (α/β: 97/3) recorded in $CDCl_3$ at 500 MHz

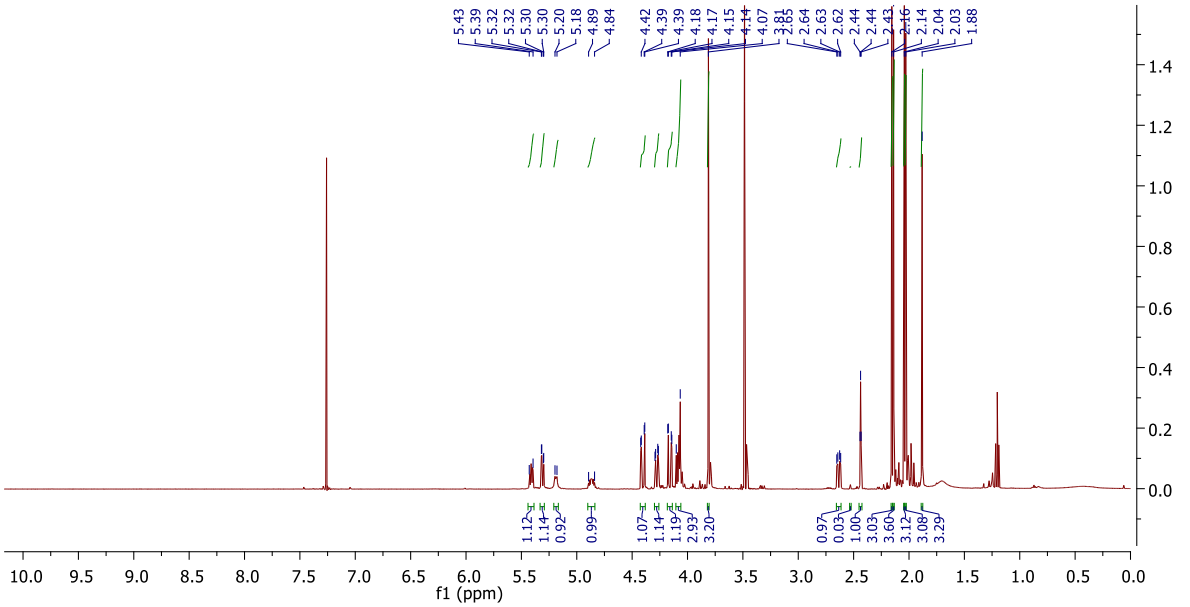

^{13}C NMR spectrum of compound 10, after recrystallization (α/β: 97/3) recorded in $CDCl_3$ at 126 MHz

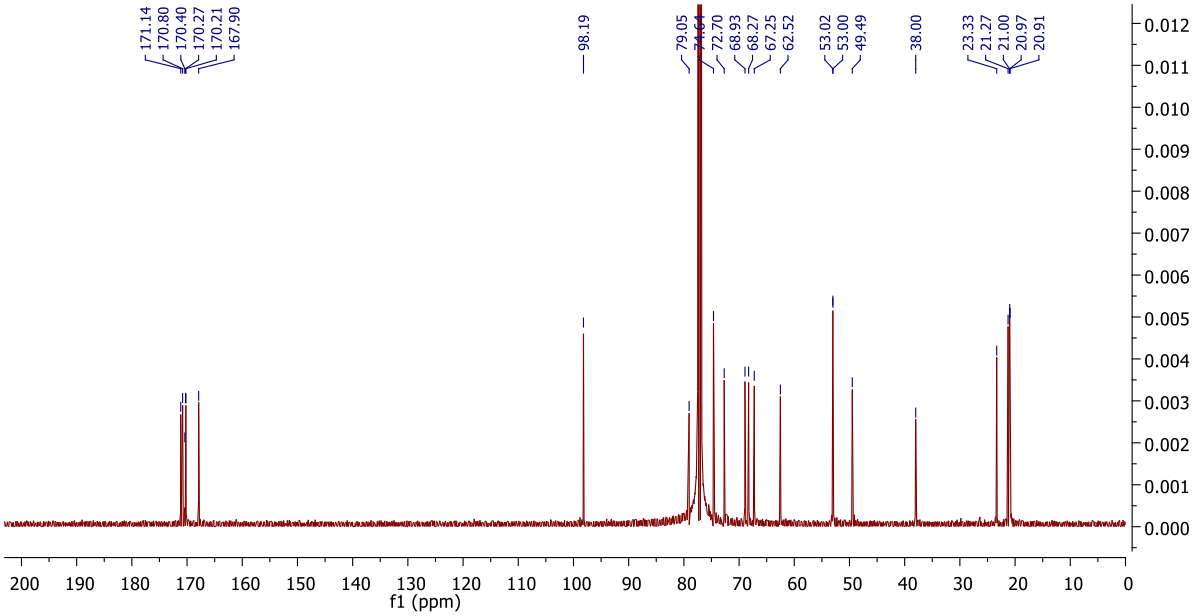

VII. Bibliography

[1] J. Yang, S. J. L. Petitjean, M. Koehler, Q. Zhang, A. C. Dumitru, W. Chen, S. Derclaye, S. P. Vincent, P. Soumillion, D. Alsteens, *Nat. Commun.* **2020**, *11*, 1–10.
[2] R. Yan, Y. Zhang, Y. Li, L. Xia, Y. Guo, Q. Zhou, *Science.* **2020**, *367*, 1444–1448.
[3] S. Beyerstedt, E. B. Casaro, É. B. Rangel, *Eur. J. Clin. Microbiol. Infect. Dis.* **2021**, *40*, 905–919.
[4] V. Yurina, *Clin. Exp. Vaccine Res.* **2020**, *9*, 169–173.
[5] S. J. L. Petitjean, W. Chen, M. Koehler, R. Jimmidi, J. Yang, D. Mohammed, B. Juniku, M. L. Stanifer, S. Boulant, S. P. Vincent, D. Alsteens, *Nat. Commun.* **2022**, *13*, 2564.
[6] W. Chen, T. Mohy El Dine, S. P. Vincent, *Chem. Commun.* **2021**, *57*, 492–495.
[7] A. Mittal, K. Manjunath, R. K. Ranjan, S. Kaushik, S. Kumar, V. Verma, *PLOS Pathog.* **2020**, *16*, 1–19.
[8] F. Li, *Annu. Rev.Virol.* **2016**, 237–264.
[9] J. Cui, F. Li, Z. L. Shi, *Nat. Rev. Microbiol.* **2019**, *17*, 181–192.
[10] T. Hu, Y. Liu, M. Zhao, Q. Zhuang, L. Xu, Q. He, *PeerJ.* **2020**, *8*, 1–30.
[11] M. Örd, I. Faustova, M. Loog, *Sci. Rep.* **2020**, *10*, 1–10.
[12] J.-D. Lelièvre, A. Gautheret-Dejean, K. Petitprez, S. Tchalkamian, Aspects Immunologiques et Virologiques de l'infection Par Le SARS-CoV-2, Report, **2020**.
[13] B. Turonová, M. Sikora, C. Schürmann, W. J. H. Hagen, S. Welsch, F. E. C. Blanc, S. von Bülow, M. Gecht, K. Bagola, C. Hörner, G. van Zandbergen, J. Landry, N. Trevisan Doimi de Azevedo, S. Mosalaganti, A. Schwarz, R. Covino, M. D. Mühlebach, G. Hummer, J. Krijnse Locker, M. Beck, *Science.* **2020**, *370*, 203–208.
[14] Sciensano, *Fact Sheet COVID-19 Disease (SARS-CoV-2 Virus)*, **2022**.
[15] M. Bosso, T. A. Thanaraj, M. Abu-Farha, M. Alanbaei, J. Abubaker, F. Al-Mulla, *Mol. Ther. - Methods Clin. Dev.* **2020**, *18*, 321–327.
[16] B. Coutard, C. Valle, X. de Lamballerie, B. Canard, N. G. Seidah, E. Decroly, *Antiviral Res.* **2020**, *176*, 104742.
[17] M. Scudellari, *Nat. Commun.* **2021**, *595*, 640–644.
[18] B. Li, L. Wang, H. Ge, X. Zhang, P. Ren, Y. Guo, W. Chen, J. Li, W. Zhu, W. Chen, L. Zhu, F. Bai, *Front. Chem.* **2021**, *9*, 659764.
[19] H. L. Nguyen, P. D. Lan, N. Q. Thai, D. A. Nissley, M. S. Li, *J. Phys. Chem.* **2020**, *124*, 7336–7347.
[20] W. Chen, Synthesis and Biological Evaluations of of Novel Pillar[5]Arene Conjugates, UNamur, PhD thesis, **2021**.
[21] M. A. Tortorici, A. C. Walls, Y. Lang, C. Wang, Z. Li, D. Koerhuis, G. J. Boons, B.-J. Bosch, F. A. Rey, R. J. de Groot, D. Veesler, *Nat. Struct. Mol. Biol.* **2019**, *26*, 481–489.
[22] J. Clayden, N. Greeves, S. Warren, *Organic Chemistry Second Edition*, **2012**.
[23] G. A. Rossi, O. Sacco, E. Mancino, L. Cristiani, F. Midulla, *Infection* **2020**, *48*, 665–669.
[24] J. Reece, L. Urry, C. Michael, S. Wasserman, P. Minorsky, R. Jackson, *Campbell Biology*, Pearson, San Francisco, CA, **2012**.
[25] M. Koehler, P. Aravamudhan, C. Guzman-Cardozo, A. C. Dumitru, J. Yang, S. Gargiulo, P. Soumillion, T. S. Dermody, D. Alsteens, *Nat. Commun.* **2019**, *10*, 1–14.
[26] S. Cecioni, A. Imberty, S. Vidal, *Chem. Rev.* **2015**, *115*, 525–561.
[27] V. I. Böhmer, W. Szymanski, B. L. Feringa, P. H. Elsinga, *Trends Mol. Med.* **2021**, *27*, 379–393.
[28] D. Cao, H. Meier, *Asian J. Org. Chem.* **2014**, *3*, 244–262.
[29] J. Zhao, W. Yang, C. Liang, L. Gao, J. Xu, A. C. H. Sue, H. Zhao, *Chem. Commun.* **2021**, *57*, 11193–11196.
[30] T. Ogoshi, T. A. Yamagishi, Y. Nakamoto, *Chem. Rev.* **2016**, *116*, 7937–8002.
[31] J. W. Steed, J. L. Atwood, *Supramolecular Chemistry*, *3rd Edition*, **2022**.

[32] T. Ogoshi, S. Kanai, S. Fujinami, T. A. Yamagishi, Y. Nakamoto, *J. Am. Chem. Soc.* **2008**, *130*, 5022–5023.
[33] T. Ogoshi, T.-A. Yamagishi, in *Calixarenes and Beyond*, **2016**, pp. 485–510.
[34] T. Ogoshi, N. Ueshima, F. Sakakibara, T. A. Yamagishi, T. Haino, *Org. Lett.* **2014**, *16*, 2896–2899.
[35] T. Ogoshi, T. Yamagishi, *Chem. Commun.* **2014**, *50*, 4776–4787.
[36] M. Xue, Y. Yang, X. Chi, Z. Zhang, F. Huang, *Acc. Chem. Res.* **2012**, *45*, 1294–1308.
[37] C. W. Sathiyajith, R. R. Shaikh, Q. Han, Y. Zhang, K. Meguellati, Y. W. Yang, *Chem. Commun.* **2017**, *53*, 677–696.
[38] N. Song, T. Kakuta, T. aki Yamagishi, Y. W. Yang, T. Ogoshi, *Chem* **2018**, *4*, 2029–2053.
[39] T. Ogoshi, R. Shiga, M. Hashizume, T. A. Yamagishi, *Chem. Commun.* **2011**, *47*, 6927–6929.
[40] H. Zhang, X. Ma, K. T. Nguyen, Y. Zhao, *ACS Nano* **2013**, *7*, 7853–7863.
[41] T. Ogoshi, T. Furuta, T. A. Yamagishi, *Chem. Commun.* **2016**, *52*, 10775–10778.
[42] Z. Zhang, B. Xia, C. Han, Y. Yu, F. Huang, *Org. Lett.* **2010**, *12*, 3285–3287.
[43] A. N. Baker, S. J. Richards, C. S. Guy, T. R. Congdon, M. Hasan, A. J. Zwetsloot, A. Gallo, J. R. Lewandowski, P. J. Stansfeld, A. Straube, M. Walker, S. Chessa, G. Pergolizzi, S. Dedola, R. A. Field, M. I. Gibson, *ACS Cent. Sci.* **2020**, *6*, 2046–2052.
[44] R. C. Larue, E. Xing, A. D. Kenney, Y. Zhang, J. A. Tuazon, J. Li, J. S. Yount, P. K. Li, A. Sharma, *Bioconjug. Chem.* **2021**, *32*, 215–223.
[45] H. C. Kolb, M. G. Finn, K. B. Sharpless, *Angew. Chemie - Int. Ed.* **2001**, *40*, 2004–2021.
[46] "Nobel Prize in Chemistry," can be found under https://www.nobelprize.org/prizes/chemistry/2022/summary/, **2022**.
[47] X. Dai, A. Böker, U. Glebe, *RSC Adv.* **2019**, *9*, 4700–4721.
[48] L. Liu, D. Cao, Y. Jin, H. Tao, Y. Kou, H. Meier, *Org. Biomol. Chem.* **2011**, *9*, 7007–7010.
[49] Y. Acikbas, M. Aksoy, M. Aksoy, D. Karaagac, E. Bastug, A. N. Kursunlu, M. Erdogan, R. Capan, M. Ozmen, M. Ersoz, *J. Incl. Phenom. Macrocycl. Chem.* **2021**, *100*, 39–54.
[50] M. Baier, J. L. Ruppertz, M. M. Pfleiderer, S. Blaum, L. Hartmann, *Chem. Commun.* **2018**, *54*, 10487–10490.
[51] S. Wolf, S. Warnecke, J. Ehrit, F. Freiberger, R. Gerardy-Schahn, C. Meier, *ChemBioChem* **2012**, *13*, 2605–2615.
[52] A. Malapelle, A. Coslovi, G. Doisneau, J. M. Beau, *Eur. J. Org. Chem.* **2007**, 3145–3157.
[53] T. Hansen, L. Lebedel, W. A. Remmerswaal, S. Van Der Vorm, D. P. A. Wander, M. Somers, H. S. Overkleeft, D. V. Filippov, J. Désiré, A. Mingot, Y. Bleriot, G. A. Van Der Marel, S. Thibaudeau, J. D. C. Codée, *ACS Cent. Sci.* **2019**, *5*, 781–788.
[54] P. O. Adero, H. Amarasekara, P. Wen, L. Bohe, D. Crich, *Chem. Rev.* **2018**, *118*, 8242–8284.
[55] R. Roy, C. A. Laferrière, *Can. J. Chem.* **1990**, *68*, 2045–2054.
[56] Z. Gan, R. Roy, *Can. J. Chem.* **2002**, *80*, 908–916.
[57] H. Ogura, K. Furuhata, S. Sato, K. Anazawa, M. Itoh, Y. Shitori, *Carbohydr. Res.* **1987**, *167*, 77–86.
[58] Y. Yao, M. Xue, X. Chi, Y. Ma, J. He, Z. Abliz, F. Huang, *Chem. Commun.* **2012**, *48*, 6505.
[59] B. Li, S. Zang, R. Liang, Y. Wu, T. C. W. Mak, *Organometallics* **2011**, *30*, 1710–1718.
[60] G. C. Daskhan, C. Pifferi, O. Renaudet, *ChemistryOpen* **2016**, *5*, 477–484.